OULU 2014
A 636

ACTA UNIVERSITATIS OULUENSIS

Päivi Kekkonen

CHARACTERIZATION OF THERMALLY MODIFIED WOOD BY NMR SPECTROSCOPY: MICROSTRUCTURE AND MOISTURE COMPONENTS

UNIVERSITY OF OULU GRADUATE SCHOOL;
UNIVERSITY OF OULU,
FACULTY OF SCIENCE,
DEPARTMENT OF PHYSICS AND CHEMISTRY

ACTA UNIVERSITATIS OULUENSIS
A Scientiae Rerum Naturalium 636

PÄIVI KEKKONEN

CHARACTERIZATION OF THERMALLY MODIFIED WOOD BY NMR SPECTROSCOPY: MICROSTRUCTURE AND MOISTURE COMPONENTS

Academic dissertation to be presented with the assent of the Doctoral Training Committee of Technology and Natural Sciences of the University of Oulu for public defence in Auditorium GO101, Linnanmaa, on 21 November 2014, at 12 noon

UNIVERSITY OF OULU, OULU 2014

Acta Univ. Oul. A 636, 2014

Supervised by
Docent Ville-Veikko Telkki
Professor Jukka Jokisaari

Reviewed by
Professor Sirkka-Liisa Maunu
Professor István Furó

Opponent
Professor Daniel Topgaard

ISBN 978-952-62-0611-0 (Paperback)
ISBN 978-952-62-0612-7 (PDF)

ISSN 0355-3191 (Printed)
ISSN 1796-220X (Online)

Cover Design
Raimo Ahonen

JUVENES PRINT
TAMPERE 2014

Kekkonen, Päivi, Characterization of thermally modified wood by NMR spectroscopy: microstructure and moisture components.
University of Oulu Graduate School; University of Oulu, Faculty of Science, Department of Physics and Chemistry
Acta Univ. Oul. A 636, 2014
University of Oulu, P.O. Box 8000, FI-90014 University of Oulu, Finland

Abstract

Wood is an essential material that has many applications in the fields of engineering, and the forest industry is particularly important in Fennoscandia. Among the various modification methods for wood, thermal modification has grown substantially over the past decades. It is an environmentally friendly method for increasing the lifetime and usability of timber. The aim of this thesis is to characterize the properties of thermally modified wood as well as to obtain new information on the changes taking place in pinewood due to the thermal modification process.

Several NMR methods were used to gain information on the effect of thermal modification on the microstructure and moisture components of *Pinus sylvestris* pinewood. Pinewood samples thermally modified at different temperatures were studied and compared to corresponding unmodified wood samples. Diffusion of water and methane was studied using pulsed-field-gradient stimulated-echo measurements to determine the highly anisotropic size distribution of pores in different cell structures of pinewood. NMR cryoporometry and relaxometry measurements were conducted to gain information on the amounts and environments of both the bound and free water absorbed into the wood samples. Cryoporometry measurements resulted in an upper limit value for the size of bound water sites and the combination of cryoporometry and relaxometry data enabled the size determination of cell wall micropores. Magnetic resonance imaging was used to visualize the spatial distribution of absorbed free water in the studied samples. Together these methods give a broad overall picture of the effects of the modification process.

The results of this work give new insight into the microstructure of thermally modified pinewood and its relationship to moisture, which is of importance for both wood science as well as industry. The applicability of the NMR techniques used here to the study of wood is also proven in this work. Using the techniques developed, it is possible to determine the optimal modification temperature, which is high enough to obtain the desired effects, but low enough not to destroy the microstructure of wood.

Keywords: cryoporometry, magnetic resonance imaging (MRI), nuclear magnetic resonance (NMR), PGSTE NMR, Pinus sylvestris, relaxometry, thermal modification, water absorption, wood

Kekkonen, Päivi, Lämpökäsitellyn puun tutkiminen NMR-spektroskopialla: mikrorakenne ja kosteus.
Oulun yliopiston tutkijakoulu; Oulun yliopisto, Luonnontieteellinen tiedekunta, Fysiikan ja kemian laitos
Acta Univ. Oul. A 636, 2014
Oulun yliopisto, PL 8000, 90014 Oulun yliopisto

Tiivistelmä

Puuta pystytään hyödyntämään useilla eri aloilla ja se on materiaalina tärkeä etenkin Fennoskandiassa merkittävälle metsäteollisuudelle. Useiden erilaisten puun käsittelymenetelmien joukossa lämpökäsittely on kasvattanut voimakkaasti suosiotaan viime vuosikymmeninä. Kyseessä on ympäristöystävällinen menetelmä, jolla voidaan pidentää puun käyttöikää sekä käytettävyyttä erilaisissa sovelluskohteissa. Tämän väitöskirjan päämääränä on ollut lämpökäsitellyn puun ominaisuuksien tutkiminen ja uuden tiedon saaminen puussa lämpökäsittelyprosessin myötä tapahtuvista muutoksista.

Työssä käytettiin useita eri NMR-menetelmiä lämpökäsitellyn mäntypuun (*Pinus sylvestris*) mikrorakenteen sekä puussa olevan kosteuden aiheuttamien vaikutusten tutkimiseksi. Työssä tutkittiin eri lämpötiloissa käsiteltyjä mäntypuunäytteitä, joita verrattiin vastaaviin käsittelemättömiin näytteisiin. Veden ja metaanin diffuusiota tutkittiin PGSTE-menetelmällä puun erittäin anisotrooppisen solurakenteen sisältämien huokosten mittojen määrittämiseksi. NMR-kryoporometria- ja -relaksometriamittaukset antoivat tietoa puuhun imeytyneen sidotun ja vapaan veden määrästä ja esiintymisympäristöstä. Kryoporometria-mittausten tuloksista saatiin yläraja sidotun veden esiintymispaikkojen koolle, ja kryoporometria- ja relaksometriamittausten tuottaman tiedon yhdistäminen mahdollisti soluseinämien mikrohuokosten koon määrittämisen. Magneettikuvausta käytettiin näytteisiin absorboituneen veden avaruudellisen jakauman määrittämiseen. Käytetyt menetelmät tarjoavat laajan kokonaiskuvan lämpökäsittelyprosessin vaikutuksista puulle.

Tämän työn tulokset antavat puutiedettä ja -teollisuutta hyödyttävää uutta tietoa lämpökäsitellyn männyn mikrorakenteesta sekä sen suhteesta kosteuteen. Väitöskirja myös osoittaa käytettyjen NMR-menetelmien soveltuvan hyvin puun tutkimiseen. Tämän tutkimuksen myötä kehitettyjen menetelmien avulla voidaan määrittää mm. optimaalinen lämpökäsittelylämpötila, joka on riittävän korkea haluttujen ominaisuuksien kannalta aiheuttamatta kuitenkaan puun mikrorakenteen hajoamista.

Asiasanat: kryoporometria, lämpökäsittely, magneettikuvaus (MRI), mänty, NMR-spektroskopia, PGSTE NMR, Pinus sylvestris, relaksometria, veden imeytyminen

Nature is painting for us,
day after day,
pictures of infinite beauty.

–John Ruskin

Acknowledgments

This work has been carried out in the NMR Research Group at the Department of Physics of the University of Oulu. I would like to thank the former and the present Head of Department, Professor Jukka Jokisaari and Professor Matti Weckström, for placing the facilities at my disposal.

I am deeply grateful to my supervisor Docent Ville-Veikko Telkki, whose ideas and comprehensive mentoring have enabled the completion of this thesis. Professor Jukka Jokisaari, who has also been my other supervisor, offered me the opportunity to work in the NMR Research Group while I was working on my Master's thesis and the majority of my knowledge of NMR stems from his lectures and those of Docent Juhani Lounila. Aapo Ylisassi and Muhammad Asadullah Javed have been intensively involved in the subprojects of this thesis; thank you for the collaboration. NMR laboratory facility manager Anu Kantola and later on her successors Susanna Ahola and Jianfeng Zhu have been an immeasurable help with the spectrometers at the NMR laboratory. Jouni Karjalainen has kindly assisted with the computational work for Paper III. Thank you all. A special thank you goes to Anne Selent, with whom I have shared not only an office but also the everyday joys and woes of the past few years. The NMR research group has been an inspiring working environment and I want to thank all the people who have worked in the group during the course of this thesis. The technical personnel at the Department of Physics Workshop are acknowledged for providing numerous practical solutions to problems concerning the experimental work.

I am grateful for the financial support from the Tauno Tönning Foundation, the Alfred Kordelin Foundation, the Finnish Cultural Foundation, the Finnish Foundation for Economic and Technical Sciences (KAUTE) and the Oulu University Pharmacy Foundation. This work would not have been possible without it.

A very special thank you goes to my family and friends. It is important to eat well, so big thanks to our lunch company. The discussions covering literally everything over lunch or a cup of coffee in Alakuppila have brightened even the hardest working days.

I also want to thank all my two- and four-legged friends with whom I have spent countless evenings in the forest airing my thoughts during the process of this work. With you I have also witnessed the beauty of nature in many forms. My

own Halo and Kaiku have taken me out even on the busiest days. Maxwell, who passed away during the process of this work, and Kelvin have reminded me every day, like only cats can, what is essential in life. The warmest thank you belongs to Jari. Without your encouragement and support this work would not have been completed. You have taken me above the clouds.

Oulu, September 2014 Päivi Kekkonen

List of Original Papers

This thesis is based on the following publications, which are referred to throughout the text by their Roman numerals:

I Kekkonen P.M., Telkki V.-V., Jokisaari J. (2009) Determining the Highly Anisotropic Cell Structures of *Pinus sylvestris* in Three Orthogonal Directions by PGSTE NMR of Absorbed Water and Methane. J. Phys. Chem. B 113: 1080–1084.

II Kekkonen P.M., Telkki V.-V., Jokisaari J. (2010) Effect of Thermal Modification on Wood Cell Structures Observed by Pulsed-Field-Gradient Stimulated-Echo NMR. J. Phys. Chem. C 114: 18693–18697.

III Kekkonen P.M., Ylisassi A., Telkki V.-V. (2014) Absorption of Water in Thermally Modified Pine Wood As Studied by Nuclear Magnetic Resonance. J. Phys. Chem. C 118: 2146–2153.

IV Javed M.A., Kekkonen P.M., Ahola S., Telkki V.-V. Magnetic Resonance Imaging Study of Water Absorption in Thermally Modified Pine Wood. Manuscript.

In Papers I and II the author was responsible for the experimental work and data analysis together with V.-V. Telkki and in Paper III with A. Ylisassi and V.-V. Telkki. The author wrote the initial versions of the manuscripts of Papers I, II and III. In Paper IV the author's main contribution was in tutoring the first author of the paper during the experimental work. The manuscript of Paper IV was also commented by the author.

Contents

1 Introduction

1.1 Background

This thesis presents work carried out to characterize the properties of thermally modified wood and the changes taking place in the thermal modification process. Various Nuclear Magnetic Resonance (NMR) spectroscopy methods are used to study the microstructure of thermally modified wood and the moisture components arising when the wood is exposed to external moisture. The range of methods applied to wood samples modified at several temperatures widens the perspective on the properties of thermally modified wood provided by earlier studies on the subject. The results of this work pave the way for more extensive work containing a wider range of samples modified at various temperatures that could be carried out to develop the thermal modification process further. Among other things, the techniques now developed enable the determination of the optimal modification temperature, which is high enough to obtain the desired effects of thermal modification, but low enough not to destroy the microstructure of wood. The applicability of various NMR methods to the study of wood is proven in this work, and their complementarity is also illustrated.

1.1.1 NMR Spectroscopy

The story of NMR spectroscopy began in 1945, when the NMR signal was observed for the first time independently by Felix Bloch in Stanford and Edward Purcell in Harvard [1, 2]. Nowadays, NMR has a wide variety of applications in chemical analysis, materials science, medical imaging, chemical engineering as well as in process and quality control [3].

In an NMR experiment a sample containing NMR active nuclei is placed in a strong, static magnetic field. The sample is irradiated with a radio frequency field that disturbs the thermal equilibrium of the nuclear spins of the sample. After the disturbance the spin system returns to the equilibrium, emitting a signal that contains information on the nuclei in the sample as well as their local environment.

In the course of almost 70 years, both NMR methods and their applications have expanded substantially. NMR can be used in the study of matter in gas, liquid and solid states, and numerous techniques providing information on the

structure and dynamics of the studied systems have been developed. Materials and phenomena span from simple chemical compounds to proteins and porous media as well as the flow of fluids and chemical reactions [3-6], to name a few. In addition to versatility, one of the biggest benefits of NMR is the non-invasive nature of the method. This non-invasiveness is exploited, for example, in magnetic resonance imaging (MRI) [7, 8], which is now a standard method for medical imaging, and also the most familiar application of NMR to the general public. The development in the field of NMR is continuous and new advances are being made all the time.

1.1.2 Wood and Thermal Modification

Wood has been an essential material in human history since the earliest civilizations. The use of wood started from the first weapons and tools built by man before the age of metals, and continued later on to buildings, furniture and boats, before extending to simple machines with the invention of the wheel.

Over the centuries, different modification methods for wood have been developed in order to increase the durability of the material and widen the spectrum of possible applications. The earliest methods included the use of olive oil and tar before the Industrial Revolution and the invention of commercial pressure treatment in the 19th century. Since then wood preservation has been a cornerstone of the wood processing industry.

During recent decades environmental aspects concerning the whole life cycle of a product have become major issues. As a renewable material, wood has many environmental benefits over non-renewable resources, but the forest and wood processing industry also has its downsides when it comes to environmental impacts. One of these is that many traditional chemical wood preservatives have a negative impact on the environment because of their toxicity. The need for environmentally friendly products made of renewable materials has created a demand for new wood modification methods [9].

The thermal modification of wood has been studied since the early 20th century, and there are records that the method was known as long ago as the Viking Age [10]. Several commercial thermal modification processes have been developed, one of the most recent being the ThermoWood process developed in Finland [9]. The method, in which wood is heated to a temperature of around 200°C for a certain period of time in the presence of steam, is used to improve the durability and dimensional stability of wood. One of the key benefits of the

method is its friendliness to the environment – no chemicals are used in the process.

1.2 Outline of the Thesis

This thesis consists of an introductory part covering the subject and the methods used to study it, as well as summaries of the research work that led to the four original publications that are attached at the end of the thesis.

In Chapter 2, the basics of nuclear magnetic resonance spectroscopy are introduced and the theoretical background of the methods used is discussed on a general level. Chapter 3 focuses on the studied subject, wood, on its structure and relationship with water. The chapter concentrates especially on *Pinus sylvestris* pinewood where possible, since it was the wood species used in the experimental work. Water is the co-star of the work. Not only is it used to probe wood in the experimental part of the work, but it also has a special relationship with wood that starts from the water-saturated environment in which wood is built up and continues in the essential physiological role that water has in a living tree. In Chapter 4, the thermal modification method is introduced and the effects it has on wood are elaborated.

In Chapters 5, 6 and 7, the experimental work of the thesis is summarized. Chapter 5 concentrates on magnetic resonance imaging, which is used in the experiments of each of Papers I-IV to illustrate the behavior of water, and, in the case of Papers I and II, also the methane absorbed in wood. MRI enables the visualization of the spatial distribution of free water in the studied samples. The focus of Paper IV is on MRI methods, although gravimetric measurements were also conducted. The MRI results of Paper IV illuminate the absorption processes in many ways, not only concentrating on simple imaging as a function of immersion time but also including T_2 relaxation time maps of absorbed water as well as the imaging of resin channels.

Chapter 6 encompasses the diffusion measurements of Papers I and II. The method for determining the anisotropic cell structure in *Pinus sylvestris* pinewood is presented in Paper I. The main result of Paper I is the determination of the dimensions of tracheid cell lumens in all three orthogonal directions using water and methane as probe fluids. The effect of thermal modification on cell structure is discussed in Paper II. It is demonstrated that thermal modification decreases the lumen dimensions up to very high modification temperatures, where the wood structure starts to decompose.

Paper III, in which NMR cryoporometry and relaxometry methods are combined to study water absorbed into wood, is covered in Chapter 7. The environments and amounts of both bound and free water in wood are discussed, and the effect of thermal modification is again considered. Several moisture components are identified by means of their T_2 relaxation times, and the sizes of bound water sites and cell wall micropores are determined.

2 Nuclear Magnetic Resonance Spectroscopy

Nuclear Magnetic Resonance (NMR) is a physical phenomenon in which nuclei in a static magnetic field, which are irradiated with radio waves of a certain frequency, absorb and re-emit energy from the radio frequency field. This phenomenon can be utilized in the investigation of the molecular properties of the matter in a method known as NMR spectroscopy. The aim of this chapter is to provide a short introduction to the theory of NMR and the particular methods that have been used in the experimental part of this work. A more detailed presentation on the basics of NMR can be found in many books [4, 5, 11-13], and the following overview is based on the book by Friebolin [4].

2.1 Basics of NMR Spectroscopy

Each nucleus *i* has a spin quantum number *I*, which is dictated by the number of protons and neutrons in the nucleus. The spin angular momentum $\boldsymbol{I}$, or simply, the nuclear spin, can be defined using the spin quantum number, and its length can be expressed as

$$|\boldsymbol{I}| = \sqrt{I(I+1)}. \tag{1}$$

Nuclei with non-zero ($I > 0$) spin also possess a magnetic moment $\boldsymbol{\mu}$ of the form

$$\boldsymbol{\mu} = \gamma\hbar\boldsymbol{I}, \tag{2}$$

where γ is the gyromagnetic ratio, which is a constant to each nuclide and $\hbar = h/2\pi$, in which h is the Planck constant ($6.6256 \cdot 10^{-3}$ Js). If γ is positive, the angular momentum vector $\boldsymbol{I}$ and the magnetic moment vector $\boldsymbol{\mu}$ are parallel, and if γ is negative, they are antiparallel. The NMR sensitivity of a nuclide is dependent on the value of the gyromagnetic ratio so that the sensitivity increases with increasing γ.

If a nucleus is placed in a static magnetic field, the magnetic moment $\boldsymbol{\mu}$ and the magnetic field $\boldsymbol{B}_0$ interact. This interaction is called the Zeeman interaction and it has the energy

$$E = -\boldsymbol{\mu} \cdot \boldsymbol{B}_0. \tag{3}$$

Choosing the z-axis of the laboratory frame parallel to the static magnetic field, the energy can be written as

$$E = -\mu_z B_0 = -\gamma\hbar I_z B_0. \tag{4}$$

Since the values of I_z are quantized, the interaction energy is also quantized and a nucleus with a spin I has $(2I+1)$ different possible energy levels. These levels are specified by the magnetic quantum number m, which can take values of $m = I, I-1,\ldots, -I$. The difference in the magnetic quantum numbers of two neighboring states is $\Delta m = \pm 1$ and this also defines the only allowed transitions. Thus the difference in energies can be expressed as

$$\Delta E = \gamma \hbar B_0. \tag{5}$$

Thus a transition between the energy levels can be induced by irradiating the nuclei with electromagnetic radiation with a corresponding frequency ν,

$$\nu = \frac{\Delta E}{\hbar} = \frac{|\gamma|}{2\pi} B_0, \tag{6}$$

which is called the Larmor frequency or resonance frequency.

The magnetic field experienced by the nuclei of the sample differs from the static magnetic field $\boldsymbol{B}_0$, due to interactions that change the magnetic field experienced by a specific nucleus. In addition to the Zeeman interaction of the magnetic moment of the nucleus and the static magnetic field, the nuclear magnetic shielding caused by the electrons surrounding the nucleus, the direct dipolar coupling and the indirect spin-spin coupling between a specific nucleus and the neighboring other nuclei, as well as the quadrupolar coupling of a quadrupolar nucleus with the electric field gradient, all have an effect on the studied nucleus. This provides the opportunity to observe the surroundings of a nucleus in an NMR experiment, since each of these interactions is reflected in the experimental NMR spectrum.

2.2 Magnetic Resonance Imaging

The use of Magnetic Resonance Imaging (MRI) in medical imaging is the largest area of application of nuclear magnetic resonance [3]. Again, a thorough introduction to the topic can be found elsewhere [7, 8], and only the basic principles of the method are presented here.

MRI provides spatial information on the sample under study. In an MRI experiment the position information is encoded to the frequency of the NMR signal by applying magnetic field gradient pulses in addition to the static magnetic field. As presented earlier, the Larmor frequency is proportional to the magnetic field experienced by the nucleus. If the strength of the magnetic field

experienced by the nuclei varies with position, this variation is observed in the Larmor frequencies of the nuclei, which can be expressed as

$$\omega(\boldsymbol{r}) = \gamma|\mathrm{B(r)}| = \gamma(|B_0| + \boldsymbol{g}\cdot\boldsymbol{r}), \tag{7}$$

where $\boldsymbol{g}$ is the gradient tensor and $\boldsymbol{r}$ is the position of the spin. A magnetic field gradient can thus be used to create an image of the sample.

In MRI, the information is sampled in the reciprocal *k*-space and the measured signal is

$$s(\boldsymbol{k}) = \int \rho(\boldsymbol{r}) e^{i2\pi\boldsymbol{k}\cdot\boldsymbol{r}} d\boldsymbol{r}, \tag{8}$$

where $\rho(\boldsymbol{r})$ is the effective spin density and $\boldsymbol{k} = (1/2\pi)\gamma\boldsymbol{g}\delta$, in which $\boldsymbol{g}$ is the gradient vector and δ is the duration of the gradient pulse. The inverse Fourier transformation translates the information from the *k*-space to the direct space, *r*-space, and thus the effective spin density can be written as

$$\rho(\boldsymbol{r}) = \int s(\boldsymbol{k}) e^{-i2\pi\boldsymbol{k}\cdot\boldsymbol{r}} d\boldsymbol{k}. \tag{9}$$

Numerous MRI methods have been developed for different purposes including imaging of flow, diffusion imaging, and functional MRI. The structure or the dynamics of the imaged subject can be resolved by using various contrast parameters, such as spin density or relaxation times, which have different values in different materials.

MRI has been used in all the subprojects discussed in this thesis, although Paper IV is the one that concentrates most strongly on the imaging of water absorbed in wood. MRI offers versatile information that also complements the results given by the other methods.

2.3 NMR Spectroscopy of Porous Materials

Many solid natural substances can be considered to be porous materials. These include rocks, soil, and many biological tissues such as bone and wood. This type of material consists of a solid frame or matrix and a network of pores. The pores are normally filled with either gas or liquid depending on the surroundings of the material. Porous materials have many applications in, for example, material science, biosciences as well as various fields of engineering.

Traditionally, porous materials have been studied using methods such as mercury porosimetry and gas adsorption. In mercury porosimetry, the pore size distribution is determined by measuring the volume of the mercury forced into the

pores as a function of pressure. Gas adsorption, on the other hand, is based on the measurement of the amount of adsorbed gas under varying gas pressure [14].

NMR spectroscopy provides various methods for studying porous materials directly or indirectly, such as cryoporometry, diffusion techniques, direct 1D, 2D and 3D imaging, and relaxometry. NMR can be used in the study of, for example, porosity, pore size distribution, pore geometry, permeability and tortuosity as well as flow and diffusion in porous media [15, 16].

In this work, wood samples are studied using several NMR methods. In Papers I and II, water and methane are used as probe fluids, and their diffusion in wood is studied using pulsed-field-gradient stimulated-echo (PGSTE) NMR in order to determine the dimensions of the wood cell structure and how they are affected by thermal modification. In Paper III, NMR cryoporometry and relaxometry are combined to gain information on water absorption in different wood cell structures as well as to determine pore size distribution in the cell walls of wood samples.

2.3.1 PGSTE NMR

If the probe fluid is confined to a solid matrix of the porous material, the matrix restricts the diffusion of the fluid molecules, and this phenomenon can be used in obtaining information of the dimensions of the pores of the matrix. NMR is suitable for studying diffusion in porous materials because the labeling of spin coherences does not affect the diffusion of molecules and because the radio waves used in NMR can also penetrate opaque samples. Pulsed-field-gradient spin-echo (PGSE) [17] and its variant pulsed-field-gradient stimulated-echo (PGSTE) [18] are standard NMR methods for measuring the self-diffusion of fluids. The most important difference between these two methods is that the relaxation attenuation of the signal is dominated by the spin-spin, or transverse, relaxation characterized by a time constant T_2 in the case of PGSE and by the spin-lattice, or longitudinal, relaxation characterized by a time constant T_1 in the case of PGSTE. The use of these methods in studying porous materials is based on the fact that the amplitude of the echo observed in the experiment decreases with the increasing displacement experienced by the molecules during the diffusion delay Δ between two gradient pulses. The PGSTE pulse sequence used in the experiments of Papers I and II is shown in Figure 1.

If the molecules of the probe fluid are confined within a rectangular box with perfectly reflecting walls, and diffusion is studied in the direction parallel to one

side of the box of length a, according to Tanner and Stejskal [19] the amplitude of the echo observed in the PGSTE experiment is

$$E(q,a) = \frac{2[1-\cos(2\pi qa)]}{(2\pi qa)^2} + 4(2\pi qa)^2 \sum_{n=1}^{\infty} exp\left(-\frac{n^2\pi^2 D\Delta}{a^2}\right) \frac{1-(-1)^n \cos(2\pi qa)}{[(2\pi qa)^2-(n\pi)^2]^2}, \quad (10)$$

where q is defined as $q = \gamma\delta g/2\pi$, in which γ is the gyromagnetic ratio of the nucleus, and δ and g are the length and amplitude of the gradient pulse, respectively. D is the molecular self-diffusion coefficient of the probe fluid, and Δ is the diffusion delay between the gradient pulses. If the sample contains a large number of rectangular pores with different sizes, and if the pore size distribution is the sum of n Gaussian functions, the observed echo amplitude can be written as

$$E_{obs} = \sum_{i=1}^{n} p_i \frac{1}{\sigma_i\sqrt{2\pi}} \int_0^{\infty} exp\left(\frac{-(a-a_i)^2}{2\sigma_i^2}\right) E(q,a)da, \quad (11)$$

where p_i, a_i, and σ_i are the portion, mean value, and standard deviation of the ith component, respectively. The pore size distribution of the studied material can be determined by measuring the echo amplitude as a function of q and fitting Equation 11 to the data points.

Not only the diffusion properties of probe fluids, as mentioned in the previous subsection, but also the measurement parameters used, have an effect on the observable pore size range. The diffusion delay Δ used in the experiment, the narrow gradient pulse approximation, and the maximum q value ($q = \gamma\delta g/2\pi$ as defined above) all affect the observable pore size range. Based on experimental experience, it is assumed that the maximum pore size observable is about 10 times larger than the root-mean-square distance traveled by the molecules, i.e. $a \leq 10\sqrt{(2D\Delta)}$, where a is the length of the rectangular box. The narrow gradient pulse approximation means that the root-mean-square distance traveled by the fluid molecules during the gradient pulse is assumed to be much smaller than the size of the box: $\sqrt{(2D\delta)} << a$. Considering the q values used, it can be assumed that the smallest observable pore size is the inverse of the maximum q value, q_{max}: $a \geq 1/q_{max}$.

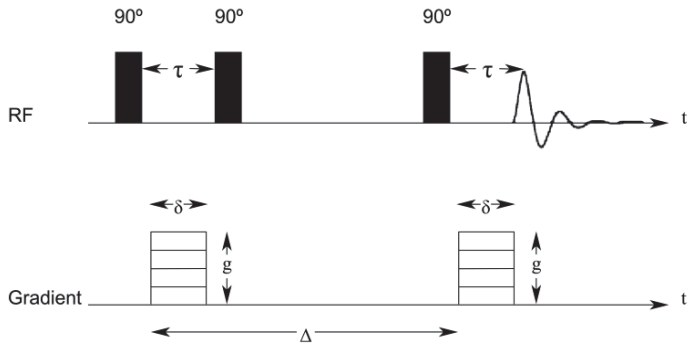

Fig. 1. PGSTE NMR pulse sequence [18].

2.3.2 NMR Cryoporometry

NMR cryoporometry enables the determination of the pore size distributions of porous materials. The melting point of a substance confined to a small pore is lower than that of the bulk substance. This lowered solid-liquid phase transition temperature is detected in NMR cryoporometry [20, 21]. The Gibbs-Thomson equation states that the melting point depression, ΔT_m, is inversely proportional to the radius, R, of the pore:

$$\Delta T_m = T_0 - T_m(R) = \frac{2\sigma_{cl}T_0}{R\Delta H_f \rho_c} = \frac{k}{R}, \tag{12}$$

where T_0 is the melting temperature of bulk liquid, T_m is the melting temperature of a cylindrical crystal with a radius R, and σ_{cl}, ΔH_f, and ρ_c are the crystal-liquid interfacial energy, the bulk enthalpy of fusion, and the density of the frozen liquid, respectively, and k is a constant that is characteristic of the probe material [22].

The melting of the substance confined to the pores of the material can be observed by measuring its ^{1}H NMR signal as a function of temperature. To detect only the signal of unfrozen liquid, a small delay needs to be applied after the excitation pulse, which gives time for the solid signal with a shorter T_2 relaxation time to decay. This can also be achieved by using the spin-echo pulse sequence. Then the integral of the measured signal is directly proportional to the amount of

unfrozen probe substance, and therefore also to the total volume of pores with a radius smaller than R corresponding to the measurement temperature T in Equation 12.

Hansen *et al*. [23] have shown that the intensity I of the liquid component as a function of the inverse temperature ($X = 1000/T$) can be written as

$$I(X) = \sum_{i=1}^{N} I_{0i}\left[1 - \mathrm{erf}\left\{(X - X_{ci})/\sqrt{2}\sigma_i\right\}\right]/2, \quad (13)$$

where

$$\mathrm{erf}(Z) = \frac{2}{\sqrt{\pi}} \int_0^Z \exp(-u^2)\mathrm{d}u, \quad (14)$$

is the so-called error function, N is the number of phase transitions, and $I_{0\mathrm{i}}$, X_{ci} and σ_{i} are the intensity, the inverse transition temperature, and the width of the temperature distribution curve of phase i, respectively. By differentiating Equation 13 with respect to the inverse temperature X, the melting point distribution curve dI/dX, which is a sum of Gaussian functions, is obtained [24, 25]. After that, using Equation 12, the pore size distribution curve can be written as

$$\frac{\mathrm{d}I}{\mathrm{d}R_p} = \frac{10^3 k_p}{\sqrt{2\pi}(R_p T_0 - k_p)^2} \sum_{i=1}^{N} \frac{I_{0i}}{\sigma_i} \times \exp\left[-\left\{\frac{10^3 R_p - X_{ci}(R_p T_0 - k_p))}{\sqrt{2}\sigma_i(R_p T_0 - k_p)}\right\}^2\right]. \quad (15)$$

Thus, the pore size distribution can be drawn by first fitting the data to Equation 13 and then inserting the obtained parameters into Equation 15.

NMR cryoporometry is suitable for determining the pore size distributions of materials whose pore sizes range from a couple of nanometers up to a few hundred nanometers. The lower limit is set by the fact that in very small pores the liquid does not freeze at all [26]. The upper limit is set by the inverse dependence between the freezing point depression of the confined substance and the pore diameter [25]. It has also been shown that there is a non-freezing surface layer of interfacial water with a thickness of 0.3-0.8 nm between the surface of the pore matrix and the solid phase of the confined substance [27]. This has to be taken into account when determining NMR cryoporometry pore size distributions in mesoporous materials quantitatively.

2.3.3 NMR Relaxometry

Fluid molecules confined to pores are subjected to interactions that change the NMR relaxation times of the fluid material. Thus the observed relaxation time distribution can also give information on the pore size distribution of the material.

The longitudinal and transverse relaxation times, T_1 and T_2, are linked to the volume-to-surface ratio V_p/S_p and further to the pore size R_p via equation [28, 29]

$$T_{1,2} = \frac{1}{\rho_{1,2}} \frac{V_p}{S_p} \alpha \frac{1}{\rho_{1,2}} R_p, \tag{16}$$

where $\rho_{1,2}$ is the surface relaxivity for longitudinal or transverse relaxation, which is dependent on the material. The model assumes that the pore size is small enough for the fluid molecule to undergo several collisions with the pore wall during the NMR timescale.

NMR relaxometry measurements are usually carried out using the Carr-Purcell-Meiboom-Gill (CPMG) method [30, 31], or some variant of it [32]. The echo amplitudes measured in the CPMG experiment can be approximated by a sum of M exponential functions [32]:

$$s_i \approx g_0 + \sum_{k=1}^{M} g_k \exp\left(-\frac{t_i}{T_k}\right), \tag{17}$$

where s_i is the signal recorded at times t_i. T_k are the relaxation times and g_k the distribution of amplitudes at relaxation times T_k, and g_0 is the value of the signal at infinite time. A relaxation time distribution can be determined by performing a Laplace inversion on the measured echo amplitudes. However, the Laplace inversion, in general, is an ill-posed problem, which means that errors in unregularized inversion are unbounded [33]. The problem can be satisfactorily circumvented by using what is known as a regularization (or smoothing) function. This can be done, for example, using the CONTIN program.

3 Wood: Structure and Moisture

Wood is formed in a living tree and its structure has evolved to fulfill the needs of the plant. Absorption of water into wood is an essential theme in this work. The relationship of wood and water is connected deeply to the physiology of plants, and understanding this relationship demands knowledge of both participants – wood and water. The following subchapters give a little insight into the structure of wood, water in a living tree, and the physical manifestation of water in wood in its various forms.

3.1 Structure of Wood

Wood can be defined as an organic polymer matrix composite built up by a living tree [34]. The structure of wood itself is inhomogeneous and as a biological material it is also susceptible to the influence of the surrounding environment. Figure 2 presents the macroscopic structure of a tree stem and Figure 3 presents the cell structure of wood on a more detailed level.

As seen in Figure 2, in the core of the tree is the pith, which runs up the tree trunk. The pith is surrounded by the xylem, which is divided into heartwood and sapwood. The inner part of the xylem is the heartwood that consists of dead cells and works as a support structure and storage for several substances. The heartwood no longer takes part in the active transport processes of the living tree. Water and minerals flow through sapwood from the roots to the leaves or needles. Growth of the tree produces concentric growth rings that can be seen in both heartwood and sapwood. The lighter rings are the earlywood that forms during the most active growth season, and the darker, denser rings are the latewood that forms during the time of slower growth. The cambium is a thin reproductive layer where cell division takes place to form new sapwood and phloem [34]. Outside of the cambium is the phloem that transports the products of photosynthesis, particularly sugars, to areas of growth and storage [35]. The outermost layer is the bark that protects the inner parts from temperature changes and dehydration [34].

Trees are divided into deciduous (angiosperm) and coniferous (gymnosperm) species that produce hardwood and softwood, respectively. In the experimental part of this work the studied material was *Pinus sylvestris* pinewood and hence the structure of softwood is emphasized in this subchapter. The microstructure of softwood is presented in Figure 3.

The size distribution of the microstructures in softwood ranges from micrometers to centimeters. Most of the structure, approximately 93%, comprises longitudinal box-like tracheid cells, also called water cells, whose task is to transport water and nutrients in the sapwood and store extracts in the heartwood. Tracheids have a hollow interior inside them called lumen. The tracheid cells are 2-4 mm in length in the longitudinal direction and their diameter is 20-30 micrometers in the transverse direction in the case of *Pinus sylvestris* pinewood. The dimensions differ slightly for early- and latewood in the radial direction where the tracheid dimensions are approximately 30 µm and 20 µm, respectively. In the tangential direction, the dimensions are the same in early- and latewood: approximately 25 µm. The volume of lumen is approximately 30% of the total tracheid volume. In latewood, the cell wall is thicker than in earlywood, and consequently the lumen volume in latewood is also smaller than in earlywood [34].

Radial rays and longitudinal resin canals form 6% and 1% of the tree volume, respectively. Both of these structures are comprised mainly of parenchyma cells, which are shorter and more prismatic than tracheid cells. Rays transport water and other liquids to the cambium, and some rays also function as resin canals. The average width of a ray without a resin canal in *Pinus sylvestris* is 20 µm in the tangential direction and 200 µm in the longitudinal direction, whereas the corresponding values for a ray with a resin canal are approximately 50 µm and 400 µm. Resin canals or resin ducts are comprised of resin-secreting parenchyma gland cells. The longitudinal resin canals are larger than those in rays, and their average dimensions in *Pinus sylvestris* are 80 µm in diameter and 50 cm in length [34].

The tracheid and parenchyma cells of softwood are connected to each other by pits on the cell wall, through which the transported elements are able to flow to neighboring cells. Pits can be either bordered, simple, or semi-bordered, depending on the structure of the closing membrane of the pit [34]. The overall diameter of bordered pits ranges from 6 to 30 µm, and again the values in earlywood are larger than those in latewood. The pit openings have a diameter of between 0.02 and 8 µm depending on the overall size of the pit [36].

The structure of hardwood is slightly more complex than that of softwood, and in hardwood water transport is mainly taken care of by vessels, which are larger structures than any of those found in softwood. Hardwood material consists of two types of tracheid cells, smaller tracheae and tube-like long fibers. Rays are also present in hardwood but, unlike softwood, there are no resin canals. Instead,

some tropical species of deciduous trees have rubber ducts which work similarly to resin canals in softwood [34].

The wood cell walls are comprised of microfibrils that form several layers [9]. The microfibrils are oriented in different directions in different layers forming a strong laminate of laminates type of structure. Because of the incomplete filling of the intermicrofibrillar region, there are void spaces called micropores on the cell walls [9]. These micropores are a few nanometers in diameter, so the term nanopore would be an illustrative alternative term for the structure. The change in the dimensions of wood due to the humidity of the environment, namely shrinking and swelling, is caused by water molecules entering the cell wall. When the cell wall is fully swollen, the micropores are open, and when water is removed from the structure in drying, the micropores collapse [9].

Chemically, the wood cell wall consists of cellulose, hemicellulose, and lignin. Cellulose, which comprises 40-50% of the wood material [9], is formed by glucose monomers polymerized into a long chain. Stiff and strong cellulose chains form microfibrils in the cell walls [34]. Hemicelluloses are heteropolysaccharides that also consist of monomers other than glucose [34]. They act as coupling agents between the microfibrils and the lignin matrix [9]. The hemicellulose content of *Pinus sylvestris* is approximately 19%. Lignin is a highly amorphous phenolic polymer that acts as the glue between microfibrils in the cell wall as well as between cell walls. Wood also contains extractives, which are organic compounds such as resins, latexes, polyphenols, and fatty acids, and inorganic compounds such as silicon dioxide, sulfuric salts, and various metallic salts [34]. The amount of extractives ranges from 0.5% up to 20% of the weight depending on the wood species [9].

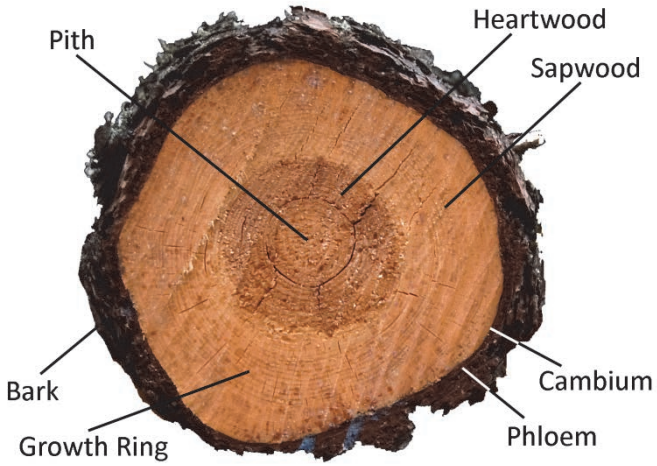

Fig. 2. Macroscopic structure of a tree stem.

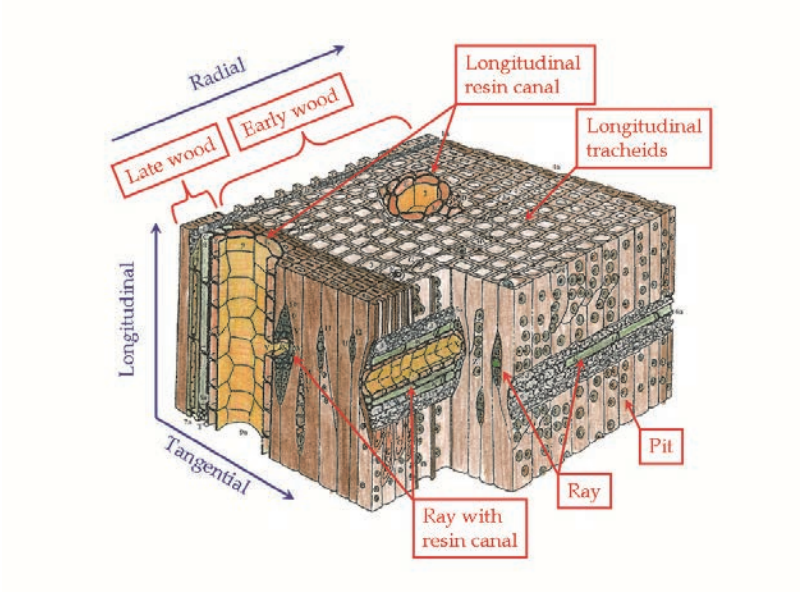

Fig. 3. Cell structure of *Pinus sylvestris* (modified after references [34] and [37]).

3.2 Wood-Water Relationship

This subchapter highlights the special relationship of wood and water. In a living tree, wood tissue has two functions: a support function enabling the tree to stand up on its own as well as to transport water and nutrients to the growing tissues of the tree. Wood is formed in an environment saturated by water, and the moisture content also has a strong effect on the properties of wood after logging.

3.2.1 Water Pathway Through the Tree

An overview of the structure of wood is aided by some background knowledge of tree physiology. The structure of wood and the functions inside the tree play even a bigger role when considering the relationship of wood and water. The following short overview on how trees work and the pathway of water through the tree is based on the book Plant Physiology by Taiz and Zeiger [35]. The intent of this overview is to give a basic understanding of the water movement in the transport channels of the tree, which is the main subject of study in the experimental part of this work.

Water is absorbed from the soil by root hairs, after which it flows through the root cortex to the xylem and then up the tree trunk to leaves or needles, where it evaporates through stomata. The ascent of water is explained by the cohesion-tension theory developed by Dixon and Joly in the 1890s [38]. Root hairs taking up water from the soil provide an enormous surface area for absorption. There are two possible types of absorption: passive absorption through osmosis and active absorption, which is dependent on the metabolic activity of the plant. The driving force of osmosis is the water potential difference across the membrane in the root hairs.

The main force that causes the water movement up the tree trunk is the transpirational pull that results from evaporation of water from the surface of the cell walls in the leaves or needles of the tree. The root pressure created by osmosis also has an impact on the water movement upwards in the trunk. The capillary action of water is caused by the adhesion of water molecules and the surface of the transport channel. Water rises in a capillary tube when it wets the walls of the tube due to adhesion. The wettability of the surface is quantified by the contact angle in which the liquid meets the solid surface. The magnitude of the capillary rise is dependent on the surface tension, the contact angle, and the

radius of the capillary. The conduits that transport water upwards through the xylem are tracheids in softwood and vessels in hardwood species.

In the leaves, water evaporates on the surface of mesophyll cell walls into air spaces inside the leaf. After that, water vapor diffuses through the air spaces in the leaf, through the stomata and across the boundary layer on the leaf surface to the outer air. The transpiration rate in the leaves depends on the water vapor concentrations of the leaf and surrounding air as well as the diffusional resistances of the stomata and the boundary layer. The difference between water vapor concentrations in the leaf and in air, namely the water vapor deficit, is the driving force of transpiration. Transpiration generates a curvature in the water menisci within the pores of the cell wall and the resulting surface tension is the reason for the transpirational pull. To put it simply, it can be stated that water movement in the plant is caused by transpiration in the leaves or needles.

3.2.2 Water in Wood

Water has several important intrinsic properties that play a large role when it is absorbed in wood. As a result of its molecular structure, hydrogen bonds between water molecules are formed. Hydrogen bonding gives rise to cohesion, which is manifested in the strong surface tension of water. Together with adhesion, cohesion also gives rise to the capillary action of water, which was already mentioned as an important factor in the water transport of plants in the previous subchapter [35].

Wood is a hygroscopic material, which means that it attracts water molecules from the surrounding environment. The moisture content (MC) of wood is commonly defined as

$$\mathrm{MC} = \frac{m_0 - m_{od}}{m_{od}} \cdot 100\%, \tag{18}$$

where m_0 is the mass of green or moist wood and m_{od} is the mass of oven-dry wood. The mass of oven-dry wood is determined for wood dried in an air oven at a temperature of 102±3°C for 24 hours [36].

Water in wood can be classified into bound water and free water. Bound water, also called hygroscopic water, exists in cell walls, and as the name suggests, it is bound via hydrogen bonds to the constituents of wood. Water molecules are bonded to the hydroxyl groups of cellulose and hemicellulose and to some extent to those of lignin as well. The amount of bound water is limited by

the number of sorption sites available for the water molecules. [36] On the other hand, water that is absorbed into the cell wall also breaks hydrogen bonds between cellulose chains, creating new sorption sites for more water molecules [39]. In the process, void spaces form between the microfibrils of the cell wall and when these voids are filled with water what is termed free bound water arises [40]. When there is only bound water present in wood, there is equilibrium between the moisture content of the wood and the relative humidity of the surrounding air. The moisture content value that wood reaches when it is exposed to a certain relative humidity and temperature for a long time is called the equilibrium moisture content (EMC). [36]

Free water, also called bulk or capillary water, exists in the large voids of the wood structure. In softwood these structures are mainly the lumens of tracheid cells and also other natural water transport channels such as rays and resin canals. Free water is held in the voids only by weak capillary forces, and it has a negligible effect on changes in the physical properties of wood, such as swelling and shrinking. Traditionally it has been stated that for free water to arise, the cell wall needs to be already saturated with bound water [36].

Fiber saturation point (FSP) is defined as the moisture content at which there is no free water but the cell walls are saturated with bound water [41]. This definition of FSP, however, is not totally accurate and it has been shown that there might be free water present although the cell walls are not totally saturated with bound water [40, 42-45]. When wood is dried below the FSP, its physical properties start to change due to the change in moisture content. Below the FSP, shrinkage and changes in mechanical strength and electrical conductivity can be observed. Above the FSP, a change in moisture content has only a slight if any effect on the properties of wood. The FSP is dependent on the wood species, but usually it is reported to be around 25-30% [36], although deviating values have been obtained using different methods: NMR studies have given a value of approximately 35% for pinewood [40], while the solute exclusion and pressure plate methods have resulted in FSP values above 40% [45, 46].

Below the FSP, the change in moisture content has a direct impact on the dimensions of wood. Wood swells when the moisture content increases and water enters the cell wall, giving rise to the bound water component. Thus the swelling takes place in the cell wall, whereas it has been determined that the change in lumen dimensions due to an increase in moisture content is negligible [36].

The change in dimensions, however, is not isotropic: in the longitudinal direction, *i.e.*, the growth direction of the tree, the change is almost negligible.

The change in dimensions is largest in the tangential direction (tangential to the growth rings when the tree is viewed as a cylinder), where it is almost double that in the radial direction. Rays present in the radial direction in softwood work as reinforcing rods, and restrict the change. The change in dimensions also has to do with the density of wood: Since swelling is caused by water entering the cell walls, latewood, which is denser and has more cell wall material than earlywood, swells more. In the radial direction the alternating early- and latewood sections even out the swelling whereas in the tangential direction the pronounced swelling of latewood forces the earlywood areas to stretch. [36]

4 Thermally Modified Wood

The forest and wood industry are significant industries worldwide, and especially in Finland and elsewhere in Fennoscandia forest-related industries account for a vast amount of industrial production. Over the last century the use of wood has proceeded from simple sawn products to engineered wood such as plywood, oriented strand board, and medium-density fiberboard (MDF). Different modification methods have also extended the variety of applications in which wood is used.

Thermal modification is an environmentally friendly method that increases the lifetime and usability of wood. Large-scale commercialization of thermally modified wood has increased since the development of the ThermoWood process. In the last ten years, the sales production of ThermoWood has risen from 20 000 m^2 in 2003 to 130 000 m^2 in 2013 [47].

4.1 Thermal Modification Process

As early as the Viking Age it was known that burning the ends of fence poles protects them from rotting. Scientific research on the thermal modification of wood began in the 1930s in Germany. During the last decades research on the subject has been carried out primarily in Europe [10].

VTT (the Technical Research Centre of Finland), together with the Finnish wood industry, has conducted comprehensive research on thermal modification and developed an industrial-scale heat-treatment process called the ThermoWood process. This licensed process consists of three phases [10]:

1. Temperature Increase and High-Temperature Drying

   The temperature of the wood is raised rapidly to around 100°C using heat and steam. After that, the temperature is further increased to 130°C for high-temperature drying, during which the moisture content of the wood decreases to nearly 0%. The duration of this phase ranges from 4 hours up to 15 hours, depending on the wood species and the earlier processing of the raw material.

2. Heat Treatment

   Following the high-temperature drying phase, the temperature is again increased to the desired heat-treatment temperature between 185°C and 215°C. The temperature is kept stable for 2-3 hours depending on the end product in which the wood will be used.

3. Cooling and Moisture Conditioning

   In the final stage, the temperature is lowered using water spray systems. When the temperature reaches 80°-90°C, re-moisturizing is conducted to set the moisture content of wood to a level of 4-7%. The cooling and conditioning phase takes 5-15 hours, depending on the heat treatment temperature used as well as on the type of processed wood material.

Altogether the ThermoWood process takes up to 36 hours, depending on the desired effect as well as on the wood species and the dimensions of the modified wood pieces. The process is suitable for both hardwood and softwood species and the raw material can be either green or kiln-dried wood. The process parameters, *e.g.* temperature and modification time, are separately optimized for different wood species and end-product purposes. This is important especially in heating and cooling to avoid the splitting and checking of the modified wood material. Steam is used as a protective gas both during drying and the actual heat treatment. It prevents the wood from burning and also accelerates the desired chemical changes that take place [10].

Thermal modification causes both chemical and physical changes in wood. The main factor in these changes is the degradation of hemicelluloses. In addition, the extractives evaporate from the wood material in the process. Other constituents, such as lignin and celluloses, start to decompose more slowly and at higher temperatures. The first changes start to appear when the temperature reaches 150°C, and temperatures above 180°C are used in the ThermoWood process [10].

4.2 Advantages of Thermal Modification

Thermal modification enhances several properties of wood, the most important being related to the decrease in the harmful effects of exposure of wood to water. Thermal modification both increases the stability of wood in changing humidity conditions and decreases the wear and decay of the material. On top of the other benefits, the method is environmentally friendly and requires only water and heat to run. However, the method has some disadvantages related to the strength properties of the produced wood material [10]. The main effects of thermal modification are compiled in Figure 4.

Thermal modification reduces the equilibrium moisture content of wood. At high modification temperatures, the decrease can be as much as 50% [10]. The absorbency of fluids to wood is also clearly reduced in the process, which can be seen in increased dimensional stability. Swelling and shrinkage due to changing moisture conditions is decreased in both the tangential and radial directions. The reduction of dimensional change due to thermal modification is normally 25-50% [10], but values of up to 80% have been reported [48].

The aforementioned changes improve the resistance of wood to the wear and decay caused by weather and biological threats, which enables the use of thermally modified wood in exterior cladding and decking. Increased biological durability was observed to be substantial, especially in the case of brown rot. ThermoWood has also been shown to be resistant to most common wood-damaging insects [10].

The heat insulation properties of wood are also improved in thermal modification, which diversifies the range of applications for thermally modified wood. It has been shown that thermal conductivity is reduced by 20-25% in the modification process [10].

The color of the material darkens with increasing modification temperature. In thermal modification the color changes throughout the material, which is a benefit compared to other modification methods that are based on impregnation of the wood material.

The effects of thermal modification that can be considered negative concern strength properties. The density of wood decreases in the modification process as a function of the modification temperature due to chemical changes as well as evaporation of extractives. The strength of the wood material correlates strongly with its density, and therefore the modification process decreases several strength properties of the material; bending, shear and splitting strengths are notably

reduced, while on the other hand compression strength seems to increase in the process. Because of these changes, thermally modified wood is not suitable for load-bearing structures. However, the change in strength properties is strongly dependent on the modification temperature, and at moderate modification temperatures the effect is significantly smaller than at high modification temperatures. Also, the possible defects of the natural material play a large role in the overall strength of the material [10].

On the other hand, the evaporation of resin in the modification process has a positive impact on the machine-tooling properties of modified wood by reducing the power requirement of the cutting equipment. Suitable working methods for thermally modified softwood are similar to those of hardwood in general [10].

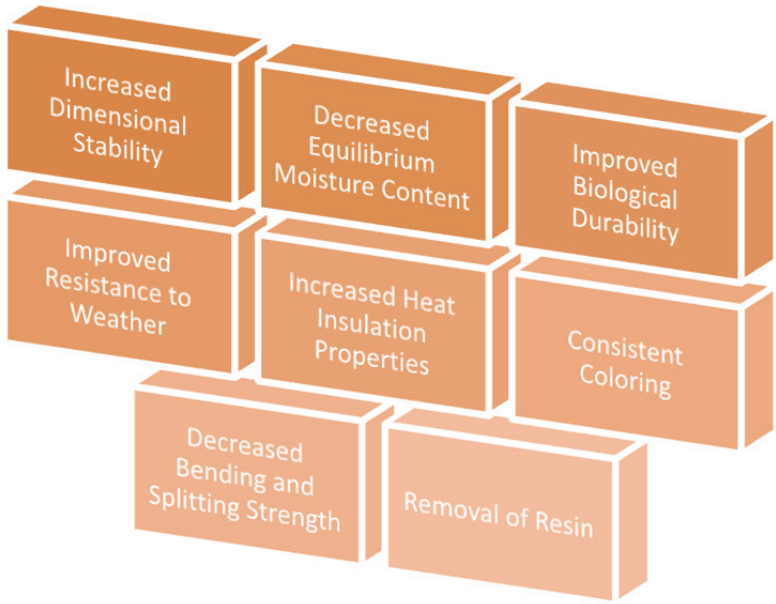

Fig. 4. Changes caused by thermal modification.

4.3 NMR Spectroscopy of Thermally Modified Wood

Earlier research on thermally modified wood using NMR spectroscopy has mainly concentrated on solid-state NMR [49]. Tjeerdsma *et al.* studied both hardwood (beech) and softwood (Scots pine) using ^{13}C Cross-Polarization Magic

Angle Spinning (CPMAS) NMR [50]. Their results clarified the chemical changes taking place in a mild two-step thermal modification process. Kosiková *et al.* studied beechwood during drying processes using both untreated wood as well as wood pre-treated by steam [51]. Their ^{13}C CPMAS NMR results indicated the formation of a lignin-cellulose complex during thermal treatment. Sivonen *et al*. used both ^{13}C CPMAS NMR and Electron Spin Resonance (ESR) spectroscopy to study thermally modified pinewood [52]. In their work, the CPMAS results indicated an increase in the relative crystallinity of cellulose as well as the destruction and deacetylation of hemicelluloses, whereas ESR showed the formation of stable free radicals, especially at thermal modification temperatures exceeding 200°C.

Liquid-state NMR has been used by Hietala *et al.*, who have studied the effect of thermal modification on pinewood with pulsed-field-gradient NMR (PFG-NMR) and ^{2}H NMR relaxation measurements [53]. The results showed that thermal modification at higher temperatures increases the T_1 relaxation time of ^{2}H and the authors interpret that it indicates increased pore size. The PFG measurements indicated that the diffusion of water is less restricted in the longitudinal direction in the tracheid cells than in the transverse direction, where the tracheid dimension was calculated to be 20 μm.

Telkki *et al.* have studied thermally modified wood with time-of-flight (TOF) remote detection (RD) MRI [54]. Hyperpolarized ^{129}Xe was used to observe the paths and dispersion of gas atoms flowing through wood samples and the results indicated that a large number of pits connecting tracheid cells are closed due to thermal modification.

5 Visualization of the Spatial Distribution of Free Water in Wood Using Magnetic Resonance Imaging

MRI was used in the experimental work in all of the original papers of this thesis. The main role of MRI has been to visualize the distribution of the probe fluids used inside the studied material and to support the measurements conducted using other NMR methods. During the course of this work, MRI has proven to be a valuable aid in monitoring the behavior of the probe fluids and also an efficient way to expand the information obtained from the studied samples.

Two-dimensional axial spin-echo images were measured at room temperature in succession with the PGSTE measurements described in Papers I and II and the cryoporometry and relaxometry measurements reported in Paper III. Paper IV focuses heavily on the use of MRI methods, providing information on the absorption of free water, related T_2 maps as well as water in resin channels, accompanied by gravimetric measurements.

5.1 High Resolution MRI of Water in Wood

In all parts of this work, ^{1}H MRI experiments were carried out using a Bruker Micro 2.5 imaging probe head with x, y and z gradients and Bruker Paravision software. The images obtained only reflect the spatial distribution of free water, since the echo time used in the MRI experiments is much longer than the T_2 relaxation times of solid wood and bound water.

In Paper I, MRI was used both to observe the absorption of the probe fluids into the wood samples as well as to ensure the correct positioning of the sample piece inside the gradient system used in the PGSTE measurements. The diameter and length of the sample pieces were 8 mm and 25 mm, respectively. MR images showed that methane, used as a probe gas, is absorbed mainly into earlywood, while water is absorbed first into latewood, and the absorption continues only later on into earlywood as well. Examples of these MR images are presented in Figure 5. MRI also indicated the structures in which pore sizes were observable with the probe fluids used in the PGSTE experiments. The images show that, in the case of water, the absorption into wood is very slow, and the wood piece is saturated by water only after several months of immersion. At an immersion time of 2 weeks, only latewood areas can be probed with water, while at an immersion

time of 2 months, some information on earlywood areas can also be gained. This was also reflected in the observed lumen dimensions given by the PGSTE measurements.

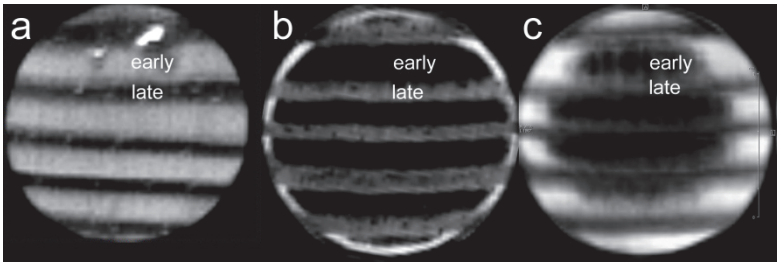

Fig. 5. MR images of the wood samples with methane (a) and water (b, c) as probe fluids. In the case of water, immersion times of 2 weeks (b) and 2 months (c) were used.

5.2 The Effect of Thermal Modification on the Absorption of Water as Observed by MRI

In Papers II and III, MRI was also used to visualize the effect of thermal modification on the absorption of water, whereas a more thorough study on the subject using samples of a different size and form was conducted in Paper IV as described in the subsequent Chapter 5.3.

In Paper II, imaging was conducted for samples containing water absorbed into wood that had been thermally modified at several temperatures (180°C, 200°C and 240°C) as well as for the respective unmodified reference samples. The samples were prepared using an immersion period of 2 weeks in distilled water before inserting the wood pieces into the sample tubes. In Paper III, the absorption was monitored over a longer period of time with MRI conducted at immersion times of 4 and 12 weeks. Apart from an additional sample that was thermally modified at 230°C, and a slightly different sample size, i.e., a diameter of 6 mm and length of 25 mm, the sample set of Paper III was similar to that used in Paper II. Henceforth, the thermally modified samples are referred to as MODX, where X is the modification temperature in Celsius degrees, and the corresponding unmodified reference samples are referred to as REFX.

The immersion time of 2 weeks used in Paper II was not long enough to produce a clear difference in the absorption of water between the thermally

modified and unmodified samples, since the overall water absorption was low. On the other hand, the results of Paper III showed clearly that when the immersion time was extended from 4 weeks to 12 weeks, full water saturation was reached in the unmodified samples. The MRI results of Paper III are shown in Figure 6. All the MR images in Figures 5 and 6 show that water is absorbed faster into latewood, where it can be observed even at the shortest immersion time of 2 weeks (Figure 5 b). However, the absorption in earlywood is visible only after 4 weeks, starting from the outer layer of the samples and extending up to full saturation at 12 weeks (Figure 6). The signal intensity is a lot stronger in earlywood than in latewood, due to the larger amount of free water absorbed as a result of the larger open lumen volume.

The results of Paper III also reveal the effect of the modification temperature on water absorption. The lowest modification temperature of 180°C does not have a visible effect on the absorption of water but at the higher temperatures the impact is clear: Modification at 200°C reduces the water absorption slightly, which can be seen as an unsaturation on sample MOD200 at the immersion time of 12 weeks. In the case of the sample modified at 240°C, the change is dramatic and the signal observed in sample MOD240 is very faint even after 12 weeks of immersion.

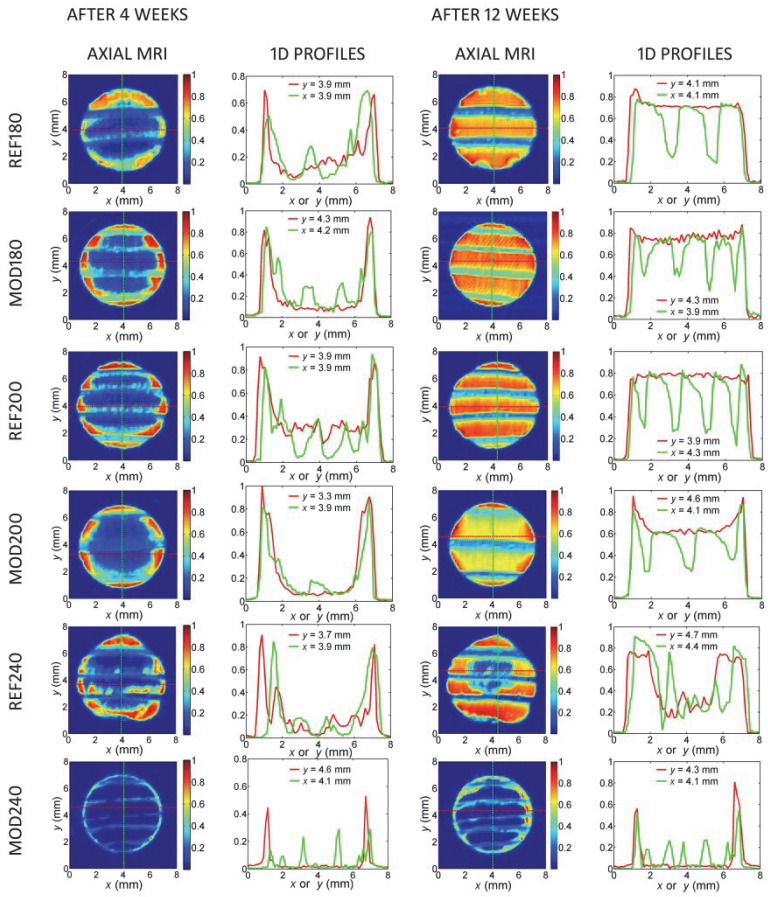

Fig. 6. Axial magnetic resonance images of both thermally modified samples as well as unmodified reference samples at immersion times of 4 and 12 weeks along with the respective 1D profiles along the tangential (red) and radial (green) directions determined from the images.

5.3 MRI Study of Absorption and T_2 Relaxation Properties of Water in Thermally Modified Wood

Paper IV concentrates on the study of water absorption in thermally modified wood samples using MRI, but gravimetric measurements were also conducted to add to the information given by MRI methods.

In the work, the absorption of water was studied in cubic wood samples thermally modified at 180°C, 200°C, 230°C, and 240°C as well as corresponding unmodified reference samples. The samples were 6 mm long on each side, and thus the dimensions were slightly smaller than in the case of the cylindrical samples used in earlier papers, where the dimensions were 6 or 8 mm in diameter and 25 mm in length. Both axial and sagittal magnetic resonance images were measured to study the absorption of water after several different immersion times. Gravimetric measurements were conducted before and after each MR imaging session to determine the moisture content and moisture per unit volume in the samples.

Immersion times of 1, 3, 7, 14, and 24 days were used in the measurements for all of the samples studied, and in the case of MOD240 the sample was also measured at an extra immersion time step of 42 days. The examples of MR images of free water presented in Figure 7 show that water is absorbed first into latewood, and only later on into earlywood as well, although at the saturated state the amount of free water in earlywood is eventually larger than that in latewood due to the larger lumen volume. This observation is in accord with the MRI results of Paper III. The images also indicate that water absorption into wood samples is reduced by thermal modification only in sample MOD240, which was modified at the highest temperature, and is not saturated with water until after 42 days of immersion. In addition, the 1D profiles along the axial direction determined from the MR images and presented on the right side of Figure 7, show that water absorption cannot be explained by a simple diffusion model using Fick's second law or the imbibition model [55], because of the complexity of wood structure.

The gravimetric measurements indicate that the absorption of water is slightly reduced by the modification temperature of 230°C, and significantly reduced by 240°C, which is in agreement with the MR results. Both the moisture content and the mass of moisture per unit volume increase with increasing immersion time, as seen in Figure 8 for the sample pair of MOD240 and REF240. When an exponential function is fitted to the measured data, a rate constant R_c is obtained, which can be used in the estimation of the change of the water absorption properties in wood due to thermal modification. The R_c values of the samples modified at or below 200°C do not differ from the corresponding values of the unmodified reference samples, whereas the value for MOD230 shows a noticeable decrease, and MOD240 a significant decrease, in the water absorption rate.

Axial MR images also reveal structures that can be interpreted as resin channels in the latewood sections of the wood samples. The resin channels can be seen in the top row images of Figure 9 as small dots, whose number in the images corresponds to the literature values for the channels. Resin channels are more easily resolved in thermally modified samples, since modification removes resin from the channels, making room for water to be absorbed.

Also presented in Figure 9 are the axial T_2 relaxation time maps obtained from the same sample set. Although Figure 9 presents only the sample pair of REF230 and MOD230 as an example, the observed T_2 values of water are larger in all the thermally modified samples as compared to the corresponding unmodified reference samples. This was deduced to be a result of the removal of resin and other extractives in the modification process.

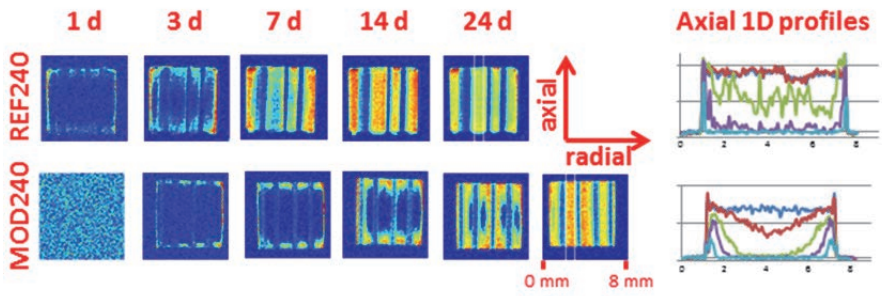

Fig. 7. Sagittal magnetic resonance images of the sample modified at 240°C and its unmodified counterpart at different immersion times. The last image showing water saturation in sample MOD240 was taken after 42 days of immersion. On the right of the MR images are the 1D profiles in the axial direction that were determined for the different immersion times.

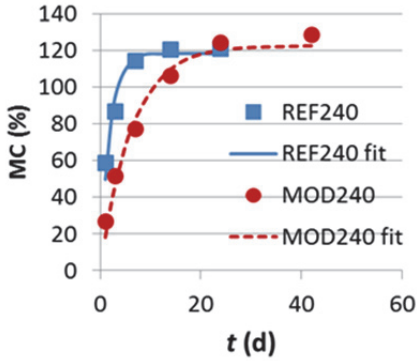

Fig. 8. Moisture content as a function of immersion time for the sample modified at 240°C and the corresponding unmodified reference sample. The solid and dashed lines represent the fits of an exponential function to the measured data.

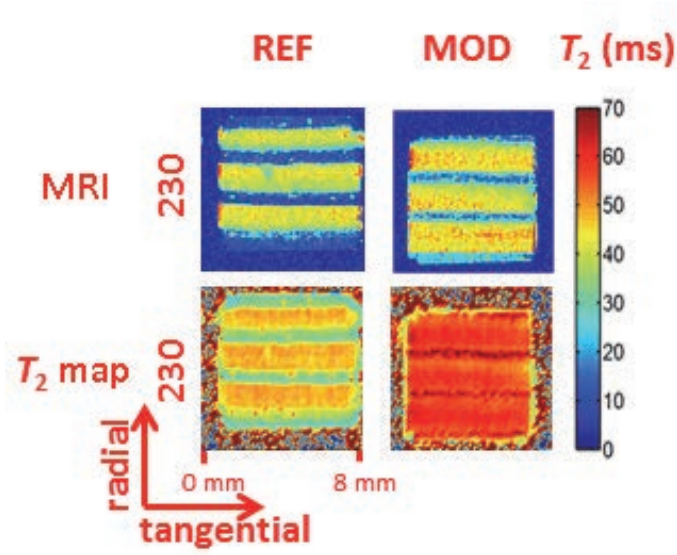

Fig. 9. Axial MR images (top row) and T_2 relaxation time maps (bottom row) for the sample modified at 230°C and its unmodified reference sample. The scale of the T_2 relaxation time values of the bottom row maps is presented on the right of the images.

6 Diffusion Measurements as a Tool in the Determination of Lumen Size

A method is presented in Paper I that uses diffusion of both liquid and gaseous probe fluids to determine the dimensions of pores in the cell structures of *Pinus sylvestris* pinewood. Water and methane, which were used as probe fluids, have significantly different diffusion coefficients, which expands the scale of the dimensions observable by PGSTE NMR to over four orders of magnitude. The method enables a more thorough characterization of the structure of wood than the previous techniques, because it enables the determination of the dimensions of the highly anisotropic cell structure in all three orthogonal directions.

In Paper II we demonstrate that the method can be used to quantify the effect of thermal modification on the microstructure of *Pinus sylvestris* pinewood. The method is applied to samples that are thermally modified at different temperatures as well as to unmodified reference samples. The results indicate that the lumen dimensions of tracheid cells decrease in all three orthogonal directions due to the thermal modification process. In addition to the diffusion measurements carried out using PGSTE NMR, this conclusion is also supported by Field Emission Scanning Electron Microscopy (FESEM) studies.

6.1 Water and Methane as Probe Fluids

The combined use of both liquid and gaseous probe fluids distinguishes this work from previous studies. Usually liquids, and especially water, have been used for determining the pore sizes of host materials, including wood [53, 56-58]. The relatively slow molecular diffusion in liquids compared to the inherent decay of their spin polarization, and enhanced relaxation of spin polarization at pore boundaries limit the pore size range that can be probed with liquids imbibed in porous materials. However, when gases are used as probe fluids, much larger dimensions can be studied because of their larger diffusion coefficient. [59]

The values used for the molecular self-diffusion coefficients D for bulk water and methane at 1.7 atm pressure were $2.04 \cdot 10^{-9}$ m^2/s and $9.83 \cdot 10^{-6}$ m^2/s, respectively. Together with the measurement parameters, as explained in Chapter 2.3.1, these D values yield a pore size range observable using water of about 10-300 μm, whereas it is from 300 μm to 10 mm for methane. Hence, water is an optimal probe for measuring the transverse dimensions of the lumens of tracheid cells that have a width of approximately 22-28 μm in earlywood and 10-15 μm in

latewood. According to the range of measurable dimensions, the widths of resin canals of approximately 80 μm, as well as rays with tangential widths of approximately 20-50 μm, could also be measured. Methane, on the other hand, is well suited for measurements in the longitudinal direction and can be used to probe the length of lumens in tracheid cells, which is approximately 2.0-3.5 mm. In case of tracheids, the lumen volume is approximately 30% of the total tracheid volume [34], and, correspondingly, the void space inside rays is significantly smaller than the height of the structure, which ranges from 200 μm to 400 μm. [34]. However, in the case of resin canals, the relative volume of the void space inside the cell structure is considerably larger than in the other structures. If a liquid with a smaller or a gas with a larger molecular self-diffusion coefficient D were used, the range of observable pore sizes would be even larger than the range achieved in this work.

In the model used in the analysis, the pores were assumed to be rectangular, which is a good approximation in the case of the lumens of tracheid cells. However, the cross-sections of pores inside rays and resin canals are cylindrical, and this may cause some inaccuracy in the results for these structures.

6.2 Determination of the Dimensions of Cell Structures in Wood

In the experimental work of Papers I and II, the wood samples were large compared to the microstructure of the wood, and contained several annual rings. Therefore a representative statistical average of the properties of wood was observed in the experiments. The sample pieces in which water was used as the probe fluid were immersed in distilled water for periods of either 2 weeks or 2 months before insertion in the NMR tube. In the case of samples in which methane was used as the probe fluid, moisture and gases were first removed from the sample in a vacuum line, after which methane gas was condensed into the sample and the tube was closed by melting it with a flame.

When thermally modified samples were compared to their unmodified counterparts in Paper II, the studied pieces were prepared so that the original locations of the thermally modified and unmodified sample pieces in the wood plank were next to each other to ensure the comparability of the results.

In the fits presented in the results of Paper I, the pore size distributions were assumed to consist of two Gaussian components. Both one- and three-component fits were also performed, but the one-component fits were significantly poorer than the two-component fits, whereas in the case of three-component fits, all of

the components could not be assigned to correspond to physical structures in the wood. The fitted parameters were the portion, p_i, mean value, a_i, and standard deviation, σ_i, of the ith component, as defined in Equation 11 in Chapter 2.3.1, which are shown for both methane and water samples in Table 1.

Table 1. The parameters resulting from the two-component fits for methane and water in unmodified pinewood samples.

direction	a_l	σ_l	p_l	a_r	σ_r	p_r
long	2.88 mm	0.78 mm	87%	0.29 mm	0.13 mm	13%
tan, 2 w	18.9 µm	4.9 µm	77%	54 µm	21 µm	23%
tan, 2 m	20.5 µm	5.2 µm	80%	50 µm	17 µm	20%
rad, 2 w	22.7 µm	7.4 µm	73%	53 µm	17 µm	27%
rad, 2 m	25.7 µm	7.8 µm	83%	54 µm	15 µm	17%

In the results of the fits given by samples in which methane was used as the probe fluid and the longitudinal dimensions of wood structures were studied, the first component was interpreted to correspond to the lengths of the lumens inside the longitudinal tracheid cells, and therefore subscript l was used in the parameter symbols. The second component was interpreted to represent the heights of the pores inside the radial rays, and thus subscript r was used. In the case of samples immersed in water, the first component (l) was associated with the widths of the lumens of longitudinal tracheids and the second component (r) with the widths of the longitudinal resin canals. Similarly to the MRI experiments discussed in the previous chapter, the bound water inside the cell walls was not observed in the diffusion measurements because of its short T_1 and T_2 relaxation times.

As can be seen in the MRI images presented in Chapter 5, water is first absorbed into latewood, whereas methane is observed in earlywood. Consequently, the pore size distributions measured by PGSTE NMR using the methane probe weight the dimensions in earlywood, whereas the water probe weights the latewood dimensions. However, after a longer immersion period, water is absorbed into earlywood as well. The early- and latewood lumens could not be separated in the fits because their pore size ranges are so close to each other. Radial rays, which could also have been observed in the transverse direction considering their diameter, did not produce their own component in the fits. This might be a result of the component being coalesced to the tracheid

component in the tangential direction and to the resin canal component in the radial direction, again due to similar pore size ranges.

The clearest observation of the values presented in Table 1 is that the average lumen size is larger in the radial direction than in the tangential direction, which is in agreement with the knowledge of softwood structure presented in Chapter 3. The absorption behavior of water, which is also seen in the MRI data as mentioned earlier, is visible when the results are analyzed as a function of immersion time. The increase in lumen dimensions in both the radial and tangential directions with increasing immersion time stems from water absorption advancing into earlywood with a larger lumen size than that of latewood, where water is absorbed first. The lumen dimension itself does not increase due to the increasing MC, since the swelling due to moisture occurs only in the cell wall.

The results presented in Table 1 also give a very large value for the portion of resin canals p_r. This is probably due to the fact that the diameter of resin canals is large compared to other structures in the wood and thus water is absorbed more easily into resin canals than into smaller structures and hence they are portrayed in a larger proportion than the other structures. The relative volume of the void space inside the resin canal to its total volume is also larger than in the case of lumens.

The diffusion of fluid molecules from one tracheid cell to another was not taken into consideration in the determination of the dimensions. Diffusion between cells was estimated to be negligible in the timescale of the PGSTE experiment [57] and the pits connecting the cells are closed when the wood is dried after cutting. In addition, the slow absorption of water into the sample that was observed using MRI indicates the minor effect of diffusion between cells.

A larger set of samples, including both wood thermally modified at different temperatures as well as unmodified reference samples, was used in Paper II. In contrast to the results of Paper I presented in Table 1, it was concluded in the analysis of the results obtained for the water samples of Paper II that one-component fits gave satisfactory results, and the fitted component reflects the width distribution of lumens. In the case of the methane samples, a two-component fit was conducted and the major component was again associated with the length of lumens. The minor component was assumed to stem from the methane in rays and residual moisture or extractives. However, since the diameter of the rays is smaller than the smallest observable dimension of the methane probe and the diffusion coefficient of the moisture or extractive molecules is

different from that of methane, only the lumen dimensions could be determined reliably.

To assess the results of the PGSTE measurements, FESEM was also used to obtain images of the wood samples. A FESEM image of one of the samples (REF180) is presented in Figure 10. The white double-headed arrows illustrate how the lumen dimensions of tracheid cells in the tangential and radial directions were determined from the images. The determination of the lumen size was only possible in the transverse direction, and only earlywood lumens were seen in the images as the latewood lumens were blocked by dust from cutting. It also has to be pointed out that the FESEM images only depict the cell structure on the surface of the sample at the imaged spot. Therefore, the FESEM results represent the local average lumen sizes in earlywood on the surface of the sample pieces whereas, in the case of the PGSTE experiments, approximately half a million tracheid cells were estimated to be inside the sample volume, giving a representative statistical average of the properties of wood. Taking the restrictions of this method into account, the average lumen dimensions given by FESEM are in accordance with the PGSTE measurements and the FESEM results also support the conclusion of the effect of thermal modification on the lumen dimension, which is discussed in the next subchapter.

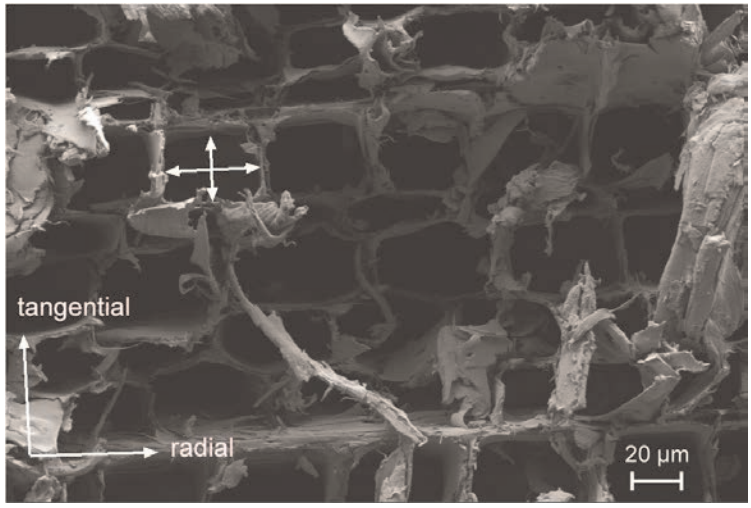

Fig. 10. FESEM image of the earlywood area of sample REF180. White double-headed arrows illustrate how the lumen dimensions of tracheid cells were determined in the tangential and radial directions.

6.3 The Effect of Thermal Modification on the Lumen Dimension

The effect of thermal modification on the wood cell structures was investigated in Paper II by comparing the pore size distributions measured from thermally modified samples to those of the respective unmodified reference samples. An example of the results of both the MRI and PGSTE measurements for samples REF240 and MOD240 are presented in Figure 11.

The main result of Paper II is that the lumen dimension decreases in all three orthogonal directions due to the thermal modification process. The percentage changes of the mean lumen dimension in different directions and for different modification temperatures are presented in Figure 12, together with the changes observed in the FESEM images taken for comparison. It is assumed that the reason for the observed decrease is that the thermal modification process closes the cell wall micropores permanently, preventing the wood from swelling even when exposed to moisture. In the case of the samples modified at 180°C and 200°C, the relative decrease was largest in the radial direction, whereas for the sample modified at 240°C, the decrease was largest in the longitudinal direction.

As seen in Figure 12, the results also indicate that the decrease is largest for the sample modified at 200°C and that, above a certain critical modification

temperature, the observed lumen size again starts to increase. This was interpreted to result from the decomposition of the structure of wood. The results imply that, above this critical temperature, the cell walls begin to disintegrate and the diffusion of the probe molecules through broken cell walls is observed as an increase of the lumen dimension in the PGSTE experiment. Also, the behavior of the standard deviation σ_l that represents the width of the lumen size distribution supports this conclusion: In the transverse directions, the standard deviation is smaller in the thermally modified samples than in the reference samples at the two lowest modification temperatures, but at the highest temperature of 240°C it becomes larger than in the respective reference sample.

Apart from some individual values, the lumen dimensions given by the FESEM images support the results of PGSTE measurements. On average, FESEM gives larger values than PGSTE, which is due to the fact that FESEM images cover only the earlywood parts, where the lumen dimensions are larger than in latewood. The deviation of individual FESEM results from the PGSTE values can be explained by the fact that FESEM measures only the local average lumen size, whereas PGSTE reflects the pore size distribution of the whole sample.

To maximize the positive effects of thermal modification in terms of dimensional stability and biological durability, the temperature used in the modification process needs to be high enough. The results obtained in Paper II can be interpreted to give an upper limit for the modification temperature after which the wood structure begins to decompose. According to the results obtained in this work, a temperature of 240°C is too high for modification. More data from samples thermally modified at different temperatures would, however, be needed in order to pinpoint the exact critical temperature for *Pinus sylvestris* pinewood.

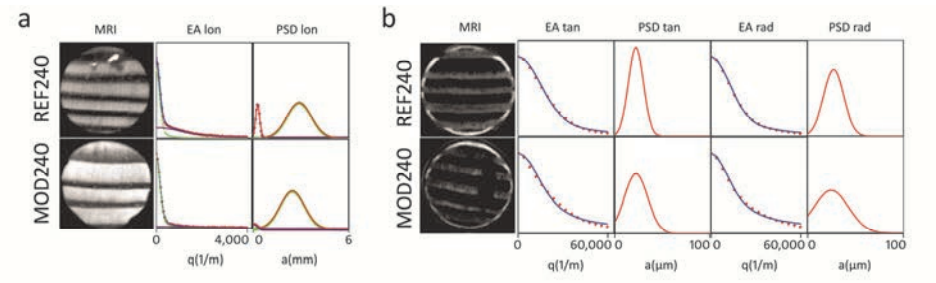

Fig. 11. Results of MRI and PGSTE experiments for samples REF240 and MOD240 with methane (a) and water (b) as probe fluids. Magnetic resonance images, PGSTE echo amplitudes (EA), as well as pore size distributions (PSD) in the longitudinal (lon) (a) and tangential (tan) and radial (rad) (b) directions are shown. In the case of methane (a) both of the two fitted components, *l* and *r*, are presented.

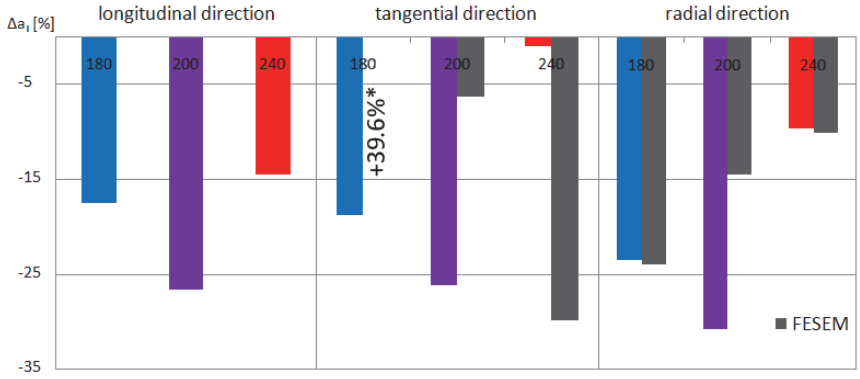

Fig. 12. Change in the mean lumen size Δa_l in the three orthogonal directions in thermal modification given by PGSTE experiments (in color) and FESEM (gray). In the case of sample MOD180 in the tangential direction, the FESEM column of positive change (+39.6%) was omitted to save plot space.

7 Combined Cryoporometry and Relaxometry Study to Assess Absorption of Water in Wood

Water absorbed into pinewood (*Pinus sylvestris*) is studied using a method that combines NMR cryoporometry and relaxometry in Paper III. In addition, MRI is used to visualize the spatial distribution of free water absorbed in wood. In NMR cryoporometry experiments, the integrals of a liquid water signal in a spin echo experiment measured both below and above the melting point of bulk water (0°C) provide information on the amounts of bound and free water absorbed into wood. NMR relaxometry, in turn, is used to reveal various non-frozen moisture components as a function of temperature. The combination of NMR cryoporometry and relaxometry also enables the determination of the micropore size distribution of the studied samples.

To investigate how thermal modification changes the water absorption properties of pinewood, the study was made using both thermally modified samples and unmodified reference samples. The results indicate that thermal modification decreases the water absorption into wood and partially blocks the access of water to cell walls, which is probably the reason for the improved dimensional stability of thermally modified wood.

7.1 Combined Cryoporometry and Relaxometry

The measurements were carried out using samples modified at several different temperatures as well as unmodified reference samples taken at corresponding locations in the original wood planks. The sample setup was similar to that used in the experiments of Papers I and II and the sample pieces were again large in relation to the microstructure of the wood and thus the early- and latewood areas were proportionally weighted. Since the intensity of the water signal is proportional to the moisture content (MC) of the wood [60, 61], the measurements were carried out using immersion times of 4 and 12 weeks in order to study the absorption of water as a function of time.

The experiments were conducted as a temperature series spanning from approximately 190 K up to room temperature in steps of 0.5 K, in order to gain information on the temperature dependence of the T_2 relaxation time distribution as well as to determine the pore sizes by means of the observed melting point

depression. Only the ^{1}H NMR signal of unfrozen water was observed in the experiments, since the T_2 relaxation times of both frozen water as well as the wood itself are much shorter than that of liquid water [42].

As discussed in Chapter 2.3.2, the pore size distributions of porous materials can be determined using NMR cryoporometry. The melting point distribution was determined using the spin-echo pulse sequence to measure the amplitude of the liquid component as a function of temperature. After this, the pore size distributions were obtained by a least squares fit of a model function to the measured integrals, as described by Aksnes *et al.* [25]. To take into account the non-freezing surface layer in the pores, a value of 0.6 nm, which is in accordance with observations by Hansen [27], was added to the NMR cryoporometry pore diameters in order to obtain the true pore sizes.

NMR relaxometry can be used to gain information on a wide variety of wood structures. Since the T_1 and T_2 relaxation times of water molecules confined to the pores of the studied material depend on their environment and mobility, the relaxation time distributions reveal different moisture components, such as bound water in the cell wall and free water in the larger cavities of the wood. In this work, T_2 relaxation time distributions were obtained by conducting CPMG (Carr-Purcell-Meiboom-Gill) [30, 31] experiments using the modified CPMG pulse sequence:

$$\left(\frac{\pi}{2}\right)_x - \tau_1 - \pi_y - \tau_1 - echo - \tau_2 - \pi_y - \tau_2 - echo - [\tau_3 - \pi_y - \tau_3 - echo]_{n-2}, \quad (19)$$

where the delays τ_1, τ_2 and τ_3 were chosen so that it was also possible to observe the rapidly decaying components. Laplace inversion was applied to the measured echo amplitudes using the CONTIN program [33]. This procedure yielded a representative T_2 relaxation time distribution of water in the samples.

Cryoporometry and relaxometry complement each other, and together they give a wide perspective on the absorption of water in wood and how it is affected by thermal modification.

7.2 The Effect of Thermal Modification on the Amount of Bound and Free Water

Spin echo experiments carried out both above and below the melting point of bulk water enable the determination of bound and free water amounts after correcting the measured signal amplitudes for Curie's law, which states that the magnetization of a material in a magnetic field is inversely proportional to temperature. At 265 K free water is frozen, and only the signal from unfrozen bound water in the cell wall is observed and thus its amplitude is proportional to the amount of bound water. Above the bulk melting point of water, both bound and free water are observed. The amount of free water can be obtained by subtracting the portion of bound water determined at 265 K from the signal observed at a temperature of 281 K.

The amounts of bound and free water as a function of modification temperature are presented in Figure 13. It can be seen in Figure 13 a and b that the absolute amounts of both bound and free water decrease when the modification temperature exceeds 200°C. The difference in the behavior of the thermally modified samples and unmodified reference samples is distinct and also consistent when the data with different immersion times are compared. In Figure 13 c and d, the relative changes in the amounts of bound and free water due to thermal modification are presented, *i.e.*, the values given by the thermally modified samples are compared to those of their unmodified counterparts. The amount of bound water decreases slightly even at the lowest modification temperatures, whereas the amount of free water decreases only at higher modification temperatures above 200°C. Although a parallel transition is observed between the two separate measurement sets where an immersion time of 4 weeks was used (labeled 4w and 4w*), the trend in the behavior is consistent and also independent of the immersion time used. The results show that the effect of the modification is larger on bound water content than on free water. This can be interpreted so that the modification partially blocks the access of water to the cell walls. This could also be the root cause of the improvement of dimensional stability in thermal modification [9].

Earlier remote detection MRI studies by Telkki *et al.* [54] have shown that thermal modification at 240°C decreases flow through the tracheid network, which implies that a large number of pits connecting the cells are closed in the modification process. The results of Paper III show a significant decrease in the amount of free water in thermally modified samples when the modification

temperature approaches 240°C. This can also be interpreted to result from the closing of pits in the thermal modification above 200°C, which prevents free water from traveling from one cell to another.

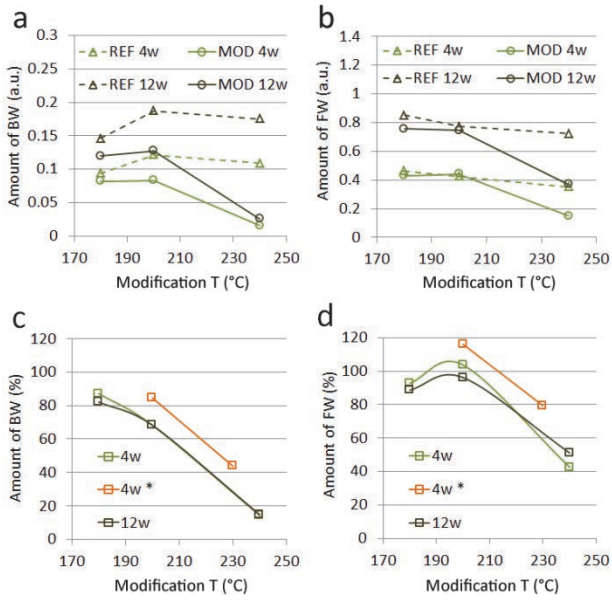

Fig. 13. Amounts of bound (BW) and free (FW) water as a function of modification temperature. The absolute amounts of bound (a) and free (b) water are presented in arbitrary units for both the thermally modified samples as well as for the respective unmodified reference samples after immersion times of 4 and 12 weeks. The relative changes due to thermal modification in the amounts of bound (c) and free water (d) are also shown. At the immersion time of 4 weeks, two separate measurement sets, labeled 4w and 4w* in the graphs, were conducted.

7.3 The Size of Bound Water Sites and Cell-Wall Micropores

When the information on pore sizes given by NMR cryoporometry measurements is connected to the T_2 relaxation time distributions given by NMR relaxometry, it is possible to calculate the pore sizes of certain wood structures.

An example of the data in the case of samples REF200 and MOD200 is presented in Figure 14. The T_2 relaxation time distributions obtained from the CPMG measurements show a total of four components. Two of the components are observed below 273 K, and are interpreted to arise from the bound water in

the cell walls. We concluded that the shorter T_2 component arises from water molecules that are hydrogen bonded to the hydroxyl groups present between the cellulose chains. The longer T_2 component is considered to originate from water in the cell wall micropores. Above 273 K, four T_2 relaxation time components can be observed. The two shortest correspond to the bound water components observed below 273 K and the two longer components are interpreted to arise from free water. The longer T_2 component of free water is connected to the tracheid lumens in earlywood whereas the other is assumed to arise from the tracheid lumens as well as ray lumens in latewood [62].

Using the data observed below the bulk melting point of water in the cryoporometry measurements enabled calculation of the pore size distribution presented on the left in Figure 15. The results give a value of 1.2−2.5 nm for the size of bound water sites both in the case of unmodified samples as well as samples thermally modified at different temperatures. It has to be pointed out that the peak observed in the pore size distribution may be affected by the decrease of the T_2 relaxation time when the temperature falls below 230 K, which decreases the signal amplitude. Thus, the pore size distribution cannot be considered to be quantitative, but it shows that the size of bound water sites is mostly below 2.5 nm.

Combining the cryoporometry and relaxometry data, it is also possible to determine the pore size distribution of the micropores by using the amplitudes of the micropore component only. The calculated micropore size distribution is presented on the right in Figure 15. The results give a value of 1.5 to 4.5 nm for the size of the micropores, which is in agreement with earlier studies conducted using other methods [9]. The decrease in the area of the micropore size distribution as a function of modification temperature also shows that the micropores are blocked in thermal modification. In addition to the amounts of bound and free water discussed earlier, this is the main result of Paper III, and to our knowledge it is the first time that NMR cryoporometry and relaxometry have been combined to obtain such information on a certain moisture component.

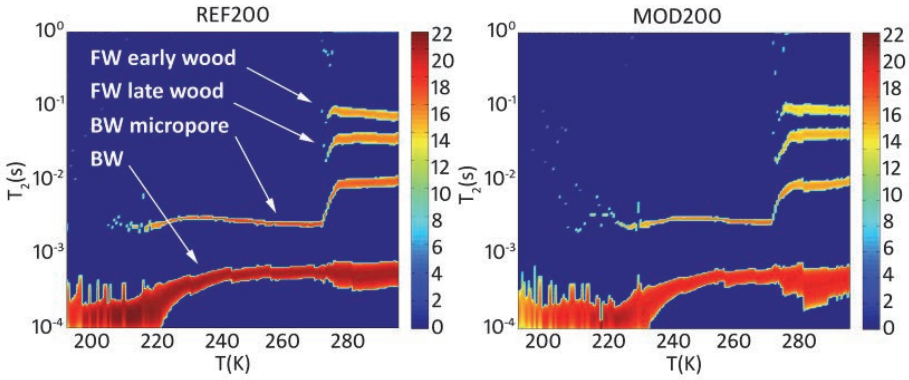

Fig. 14. T_2 relaxation time distributions as a function of temperature for samples REF200 (left) and MOD200 (right). In both samples components can be observed that arise from bound water, water in micropores and free water in early- as well as latewood.

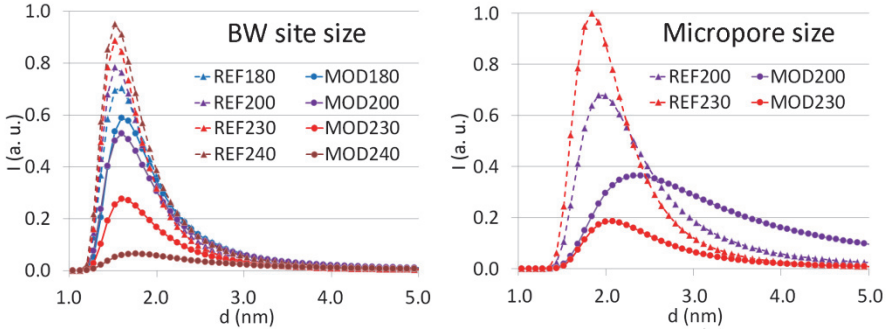

Fig. 15. Pore size distributions in both thermally modified as well as unmodified reference samples determined for bound water sites (left) and micropores (right).

8 Conclusions

This thesis demonstrates the versatility of NMR spectroscopy in the study of wood. In this work, several NMR methods were used to gain information on the microstructure and moisture components in wood with a focus on the effect of thermal modification. Changes caused by thermal modification were analyzed using pinewood samples that had been thermally modified at different temperatures.

Papers I and II concentrated on the microstructure of wood. A method utilizing PGSTE NMR to measure the dimensions of cell structures in wood was presented in Paper I. It was demonstrated that by combining liquid and gaseous probe materials, the range of observable pore sizes is expanded to more than 4 orders of magnitude. In this work, water and methane were used as probe fluids to determine pore sizes on a scale from 10 μm to 10 mm. In pinewood, this range covered all three orthogonal dimensions of lumens in tracheid cells as well as the longitudinal dimension of radial rays and the transverse dimension of resin canals. The range of observable dimensions could be expanded even further using a probe liquid with a smaller diffusion coefficient or gas with a larger diffusion coefficient.

In Paper II, the method was used to study changes in pinewood cell structure due to thermal modification. The results indicated that the lumen size decreases in all three orthogonal directions in the thermal modification process. The behavior of lumen size as a function of modification temperature also indicated that at lower modification temperatures the decrease in lumen dimensions becomes larger with temperature but that after a critical temperature the lumen size again begins to increase. It was concluded that the behavior above the critical temperature is due to decomposition of the cell wall structure, which enables the probe material to diffuse through broken cell walls, producing a larger pore size in the measurements. The critical modification temperature was determined to be around 200°C, but defining the exact temperature for pinewood would call for similar measurements of samples modified at several temperatures around 200°C. The method itself proved advantageous in studying the changes taking place in thermal modification and may be of use in improving the thermal modification process.

The absorption of water into wood was another central theme in this work. In Paper III, the behavior of water in thermally modified wood samples was studied using NMR cryoporometry and relaxometry. The measurements conducted both

below and above the melting point of bulk water showed four separate moisture components in the measured T_2 relaxation time distributions: Bound water in cell walls and in cell wall micropores, as well as free water in the tracheid lumens of earlywood and latewood could be distinguished. The size of bound water sites as well as the size of micropores could be obtained by combining the cryoporometry and relaxometry results. The results also indicated that thermal modification has a clear effect on the absorption of water into wood. The amount of free water is decreased when the modification temperature exceeds 200°C, whereas in the case of bound water, modification even at a temperature of 180°C reduces absorption into the cell walls. The results can be interpreted to imply that thermal modification partially blocks the access of water into the cell wall, thus increasing the dimensional stability of wood. Modification at higher temperatures also closes a large number of the pits that connect tracheid cells, reducing free water absorption.

MRI has been an efficient tool in all of the experimental work performed in the course of this project. In particular, the results of Paper IV provide versatile information on the behavior of free water in wood samples, both as a function of immersion time and of modification temperature. The MRI results imply that absorption of free water is significantly reduced only at the highest modification temperature used of 240°C. The effect of thermal modification was also seen in the T_2 relaxation time values determined from the samples that were most probably influenced by the removal of resin and extractives due to thermal modification. Individual resin channels could also be identified in the images. In addition, it was shown that water absorption into wood cannot be explained by a simple diffusion model.

The results of this work have given new insight into the changes taking place in the thermal modification of pinewood. The use of a combination of various methods has helped in creating an overall picture of the effects of the modification process. More specific information could be obtained by extending the methods used to a wider range of thermal modification temperatures as well as to other wood species in addition to *Pinus sylvestris* pinewood.

References

1. Bloch F., Hansen W., Packard M. (1946) Nuclear Induction. Phys. Rev. 69: 127.
2. Purcell E.M., Torrey H.C., Pound R.V. (1946) Resonance Absorption by Nuclear Magnetic Moments in a Solid. Phys. Rev. 69: 37–38.
3. Blümich B. (2005) Essential NMR. Springer-Verlag, Berlin, Heidelberg, Germany.
4. Friebolin H. (1991) Basic One- and Two-Dimensional NMR Spectroscopy. VCH Verlagsgesellschaft mbH, Weinheim, Germany.
5. Keeler J. (2007) Understanding NMR Spectroscopy. John Wiley & Sons, Chichester, UK.
6. Cavanagh J., Fairbrother W.J., Palmer III A.G., Rance M., Skelton N.J. (1995) Protein NMR Spectroscopy. Academic Press Inc., San Diego, U.S.A.
7. Haacke E.M., Brown R.W., Thompson M.R., Venkatesan R. (1999) Magnetic Resonance Imaging. Physical Principles and Sequence Design. John Wiley & Sons Inc., New York, U.S.A.
8. Stapf S., Han S.-I. (2006) NMR Imaging in Chemical Engineering. Wiley-VCH, Weinheim, Germany.
9. Hill C.A.S. (2006) Wood Modification – Chemical, Thermal and Other Processes. Wiley, Chichester, UK.
10. ThermoWood Handbook. (2003) International Thermowood Association, URI: http://files.kotisivukone.com/en.thermowood.kotisivukone.com/tiedostot/tw_handbook_080813.pdf. Cited 2014/6/18.
11. Abragam A. (1961) The Principles of Nuclear Magnetism. Oxford University Press, Oxford, UK.
12. Ernst R.R., Bodenhausen G., Wokaun A. (1987) Principles of Nuclear Magnetic Resonance in One and Two Dimensions. Oxford University Press, New York, U.S.A.
13. Levitt M.H. (2001) Spin Dynamics: Basics of Nuclear Magnetic Resonance. Wiley, West Sussex, UK.
14. Dullien F.A.L. (1992) Porous Media: Fluid Transport and Pore Structure, 2nd Edition. Academic Press, San Diego, U.S.A.
15. Webber J.B.W. (2000) Ph. D. Thesis: Characterizing Porous Media. University of Kent.
16. Song Y.-Q. (2007) Novel NMR Techniques for Porous Media Research. Cem. Concr. Res. 37: 325–328.
17. Stejskal E.O., Tanner J.E.J. (1965) Spin Diffusion Measurements: Spin Echoes in the Presence of a Time-Dependent Field Gradient. Chem. Phys. 42: 288–292.
18. Tanner J.E.J. (1970) Use of the Stimulated Echo in NMR Diffusion Studies. Chem. Phys. 52: 2523–2526.
19. Tanner J.E., Stejskal E.O.J. (1968) Restricted Self-Diffusion of Protons in Colloidal Systems by the Pulsed-Gradient, Spin-Echo Method. Chem. Phys. 49: 1768–1777.
20. Mitchell J., Webber J.B.W., Strange J.H. (2008) Nuclear Magnetic Resonance Cryoporometry. Phys. Rep. 461: 1–36.

21. Petrov O.V., Furó, I. (2009) NMR Cryoporometry: Principles, Applications and Potential. Prog. Nucl. Magn. Reson. Spectrosc. 54: 97–122.
22. Jackson C.L., McKenna G.B. (1990) The Melting Behavior of Organic Materials Confined in Porous Solids. J. Chem. Phys. 93: 9002–9011.
23. Hansen E. W., Schmidt R., Stöcker M. (1996) Pore Structure Characterization of Porous Silica by 1H NMR Using Water, Benzene, and Cyclohexane as Probe Molecules. J. Phys. Chem. 100:11396–11401.
24. Schmidt R., Hansen E.W., Stöcker M., Akporiaye D., Ellestad O.H. (1995) Pore Size Determination of MCM-41 Mesoporous Materials by Means of ^{1}H NMR Spectroscopy, N_2 Adsorption, and HREM. A Preliminary Study. J. Am. Chem. Soc. 117: 4049–4056.
25. Aksnes D.W., Førland K., Kimtys, L. (2001) Pore Size Distribution in Mesoporous Materials as Studied by ^{1}H NMR. Phys. Chem. Chem. Phys. 3: 3203–3207.
26. Morishige, K.; Kawano, K. Freezing and Melting of Water in a Single Cylindrical Pore: The Pore-Size Dependence of Freezing and Melting Behavior. J. Chem. Phys. 1999, 110, 4867−4872.
27. Hansen E.W., Stöcker M., Schmidt R. (1996) Low-Temperature Phase Transition of Water Confined in Mesopores Probed by NMR. Influence on Pore Size Distribution. J. Phys. Chem. 100: 2195–2200.
28. Stallmach F., Kärger J. (1999) The Potentials of Pulsed Field Gradient NMR for Investigation of Porous Media. Adsorption 5: 117–133.
29. Brownstein K.R., Tarr C.E. (1979) Importance of Classical Diffusion in NMR Studies of Water in Biological Cells. Phys. Rev. A 19: 2446–2453.
30. Carr H.Y., Purcell E.M. (1954) Effects of Diffusion on Free Precession in Nuclear Magnetic Resonance Experiments. Phys. Rev. 94: 630–638.
31. Meiboom S., Gill, D. (1958) Modified Spin-Echo Method for Measuring Nuclear Relaxation Times. Rev. Sci. Instrum. 29: 688–691.
32. Borgia G.C., Brown R.J.S., Fantazzini P. (1998) Uniform-Penalty Inversion of Multiexponential Decay Data. J. Magn. Res. 132: 65–77.
33. Provencher S.W.A. (1982) Constrained Regularization Method for Inverting Data Represented by Linear Algebraic or Integral Equations. Comput. Phys. Commun. 27: 213–227.
34. Kettunen P.O. (2006) Structure and Properties of Wood. Trans Tech Publications Ltd, Switzerland.
35. Taiz L., Zeiger E. (2010) Plant Physiology, 5th Edition. Sinauer Associates Inc., U.S.A.
36. Siau J.F. (1984) Transport Processes in Wood. Springer-Verlag, Berlin, Heidelberg, Germany.
37. Howard E.T., Manwiller F.G. (1969) Anatomical Characteristics of Southern Pine Stemwood. Wood Sci. 2: 77–86.
38. Dixon H., Joly, J. (1894) On the Ascent of Sap. Ann. Bot. 8: 468–470.
39. Hartley I.D., Kamke F.A., Peemoeller H. (1992) Cluster Theory for Water Sorption in Wood. Wood Sci. Technol. 26: 83–99.

40. Telkki V.-V., Yliniemi M., Jokisaari J. (2013) Moisture in Softwoods: Fiber Saturation Point, Hydroxyl Site Content, and the Amount of Micropores as Determined from NMR Relaxation Time Distributions. Holzforschung 67: 291–300.
41. Tiemann D. (1907) Effect of Moisture upon the Strength and Stiffness of Wood. Bulletin 70, US Department of Agriculture Forest Services, Washington D.C., U.S.A.
42. Menon R.S., MacKay A.L., Hailey J.R.T., Bloom M., Burgess A.E., Swanson J.S. (1987) An NMR Determination of the Physiological Water Distribution in Wood During Drying. J. Appl. Polym. Sci. 33: 1141–1155.
43. Araujo C.D., MacKay A.L., Hailey J.R.T., Whittall K.P. (1992) Proton Magnetic Resonance Techniques for Characterization of Water in Wood: Application to White Spruce. Wood Sci. Technol. 26: 101–113.
44. Almeida G., Hernández R.E. (2006) Changes in Physical Properties of Tropical and Temperate Hardwoods Below and Above the Fiber Saturation Point. Wood Sci. Technol. 40: 599–613.
45. Hoffmeyer P., Engelund E.T., Thygesen L.G. (2011) Equilibrium Moisture Content (EMC) in Norway Spruce During the First and Second Desorptions. Holzforschung 65: 875–882.
46. Hill C.A.S. (2008) The Reduction in the Fiber Saturation Point of Wood due to Chemical Modification Using Anhydride Reagents: a Reappraisal. Holzforschung 62: 423–428.
47. ThermoWood Production Statistics 2013. International ThermoWood Association, URI: http://files.kotisivukone.com/en.thermowood.kotisivukone.com/tiedostot/productionstatistics2013.pdf. Cited 2014/6/18.
48. Viitaniemi P., Jämsä S. (1996) Modification of Wood with Heat Treatment. VTT Julkaisuja – Publikationer 814, Espoo, Finland.
49. Maunu S.L. (2002) NMR Studies of Wood and Wood Products. Prog. Nucl. Magn. Reson. Spectrosc. 40: 151–174.
50. Tjeerdsma B., Boonstra M., Pizzi A., Tekely P., Militz H. (1998) Characterization of Thermally Modified Wood: Molecular Reasons for Wood Performance Improvement. Holz Roh-Werkst. 56: 149–153.
51. Kosiková B., Hricovíni M., Cosentino C. (1999) Interaction of Lignin and Polysaccharides in Beech Wood (Fagus Sylvatica) During Drying Processes. Wood Sci. Technol. 33: 373–380.
52. Sivonen H., Maunu S.L., Sundholm F., Jämsä S., Viitaniemi P. (2002) Magnetic Resonance Studies of Thermally Modified Wood. Holzforschung 56: 648–654.
53. Hietala S., Maunu S.L., Sundholm F., Jämsä S., Viitaniemi P. (2002) Structure of Thermally Modified Wood Studied by Liquid State NMR Measurements. Holzforschung 56: 522–528.
54. Telkki V.-V., Saunavaara J., Jokisaari J. (2010) Time-of-Flight Remote Detection MRI of Thermally Modified Wood. J. Magn. Reson. 202: 78–84.
55. Gombia M., Bortolotti V., Brown R.J.S., Camaiti M., Fantazzini P. (2008) Models of Water Imbibition in Untreated and Treated Porous Media Validated by Quantitative Magnetic Resonance Imaging. J. Appl. Phys. 103: 094913.

56. Wycoff W., Pickup S., Cutter B., Miller W., Wong T.C. (2000) The Determination of the Cell Size in Wood by Nuclear Magnetic Resonance Diffusion Techniques. Wood Fiber Sci. 32: 72–80.
57. Johannessen E.H., Hansen E.W., Rosenholm J.B. (2006) Fluid Self-Diffusion in Scots Pine Sapwood Tracheid Cells. J. Phys. Chem. B 110: 2427–2434.
58. Meder R., Codd S.L., Franich R.A., Callaghan P.T., Pope J.M. (2003) Observation of Anisotropic Water Movement in Pinus radiata D. Don Sapwood Above Fiber Saturation Using Magnetic Resonance Micro-Imaging. Holz Roh. Werks. 61: 251–256.
59. Mair R.W., Wong G.P., Hoffman D., Hürlimann M.D., Patz S., Schwartz L.M., Walsworth R.L. (1999) Probing Porous Media with Gas Diffusion NMR. Phys. Rev. Lett. 83: 3324–3327.
60. Sharp A.R., Riggin M.T., Kaiser R., Schneider M.H. (1978) Determination of Moisture Content of Wood by Pulsed Nuclear Magnetic Resonance. Wood Fiber Sci. 10: 74–81.
61. Riggin M.T., Sharp A.R., Kaiser R. (1979) Transverse NMR Relaxation of Water in Wood. J. Appl. Polym. Sci. 23: 3147–3154.
62. Menon R.S., MacKay A.L., Flibotte S., Hailey J.R.T. (1989) Quantitative Separation of NMR Images of Water in Wood on the Basis of T_2. J. Magn. Reson. 82: 205–210.

Original Papers

I Reprinted with permission from Kekkonen P.M., Telkki V.-V., Jokisaari J. (2009) Determining the Highly Anisotropic Cell Structures of *Pinus sylvestris* in Three Orthogonal Directions by PGSTE NMR of Absorbed Water and Methane. J. Phys. Chem. B 113: 1080–1084. Copyright 2009 American Chemical Society.

II Reprinted with permission from Kekkonen P. M., Telkki V.-V., Jokisaari J. (2010) Effect of Thermal Modification on Wood Cell Structures Observed by Pulsed-Field-Gradient Stimulated-Echo NMR. J. Phys. Chem. C 114: 18693–18697. Copyright 2010 American Chemical Society.

III Reprinted with permission from Kekkonen P. M., Ylisassi A., Telkki V.-V. (2014) Absorption of Water in Thermally Modified Pine Wood As Studied by Nuclear Magnetic Resonance. J. Phys. Chem. C 118: 2146–2153. Copyright 2014 American Chemical Society.

IV Reprinted with permission from Javed M.A., Kekkonen P.M., Ahola S., Telkki V.-V. Magnetic Resonance Imaging Study of Water Absorption in Thermally Modified Pine Wood. Manuscript.

The original publications are not included in the electronic version of the dissertation.

618. Rodríguez, Pilar (2013) Combining lean thinking and agile software development : how do software-intensive companies use them in practice?

619. Vatka, Emma (2014) Boreal populations facing climatic and habitat changes

620. Isomursu, Marja (2014) Host–parasite interactions of boreal forest grouse and their intestinal helminth parasites

621. Ponnikas, Suvi (2014) Establishing conservation management for avian threatened species

622. Matusek, Florian (2014) Selective privacy protection for video surveillance

623. Virtanen, Elina (2014) Effects of haulm killing and gibberellic acid on seed potato (*Solanum tuberosum L.*) and techniques for micro- and minituber production in northern latitudes

624. Kopatz, Alexander (2014) Genetic structure of the brown bears (*Ursus arctos*) in Northern Europe

625. Loukola, Olli (2014) Information networks among species : adaptations and counter-adaptations in acquiring and hiding information

626. Langrial, Sitwat (2014) Exploring the influence of persuasive reminders and virtual rehearsal on the efficacy of health behavior change support system

627. Jaakkonen, Tuomo (2014) Intra- and interspecific social information use in nest site selection of a cavity-nesting bird community

628. Päätalo, Heli (2014) Stakeholder interactions in cross-functional productization : the case of mobile software development

629. Koskela, Timo (2014) Interaction in asset-based value creation within innovation networks : the case of software industry

630. Stibe, Agnis (2014) Socially influencing systems : persuading people to engage with publicly displayed Twitter-based systems

631. Sutor, Stephan R. (2014) Large-scale high-performance video surveillance

632. Niskanen, Alina (2014) Selection and genetic diversity in the major histocompatibility complex genes of wolves and dogs

633. Tuomikoski, Sari (2014) Utilisation of gasification carbon residues : activation, characterisation and use as an adsorbent

634. Hyysalo, Jarkko (2014) Supporting collaborative development : cognitive challenges and solutions of developing embedded systems

Book orders:
Granum: Virtual book store
http://granum.uta.fi/granum/

UNIVERSITY OF OULU P.O. Box 8000 FI-90014 UNIVERSITY OF OULU FINLAND

ACTA UNIVERSITATIS OULUENSIS

ISBN 978-952-62-0611-0 (Paperback)
ISBN 978-952-62-0612-7 (PDF)
ISSN 0355-3191 (Print)
ISSN 1796-220X (Online)

UNIVERSITY of OULU
OULUN YLIOPISTO